Available online at www.sciencedirect.com

ScienceDirect

Nuclear Physics B 995 (2023) 116349

NUCLEAR PHYSICS B

www.elsevier.com/locate/nuclphysb

High Energy Physics – Phenomenology

Semileptonic decays $D \to P/V/S\ell^+\nu_\ell$ with the SU(3) flavor symmetry/breaking

Ru-Min Wang [a,*], Yue-Xin Liu [a], Meng-Yuan Wan [a], Chong Hua [a], Jin-Huan Sheng [b], Yuan-Guo Xu [a]

[a] College of Physics and Communication Electronics, Jiangxi Normal University, Nanchang, Jiangxi 330022, China
[b] School of Physics and Engineering, Henan University of Science and Technology, Luoyang, Henan 471000, China

Received 8 June 2023; received in revised form 18 August 2023; accepted 31 August 2023
Available online 6 September 2023
Editor: Hong-Jian He

Abstract

Many exclusive $c \to d/s\ell^+\nu_\ell$ ($\ell = e, \mu, \tau$) transitions have been well measured, and they can be used to test the theoretical calculations. Motivated by this, we study the $D \to P/V/S\ell^+\nu_\ell$ decays induced by the $c \to d/s\ell^+\nu_\ell$ transitions with the SU(3) flavor symmetry approach, where P denotes the pseudoscalar meson, V denotes the vector meson, and S denotes the scalar meson with a mass below 1 GeV. The different decay amplitudes of the $D \to P\ell^+\nu_\ell$, $D \to V\ell^+\nu_\ell$ or $D \to S\ell^+\nu_\ell$ decays can be related by using the SU(3) flavor symmetry and by considering the SU(3) flavor breaking. Using relevant data, we predict the not yet measured or not yet well measured processes in the $D \to P/V/S\ell^+\nu_\ell$ decays. We find that the SU(3) flavor symmetry approach works well in the $D \to P/V\ell^+\nu_\ell$ decays. Many branching ratios of the $D \to S\ell^+\nu_\ell$ decays are predicted by using the data of the $D_s^+ \to f_0(980)e^+\nu_e$ and $D \to S(S \to P_1P_2)\ell^+\nu_\ell$ decays, in addition, the two quark and the four quark scenarios for the light scalar mesons are analyzed. The SU(3) flavor symmetry predictions of the $D \to S\ell^+\nu_\ell$ decays need to be further tested, and our predictions of the $D \to S\ell^+\nu_\ell$ decays are useful for probing the structure of light scalar mesons. Our results in this work could be used to test the SU(3) flavor symmetry approach in the semileptonic D decays by the future experiments at BESIII, LHCb and BelleII.

* Corresponding author.
E-mail addresses: ruminwang@sina.com (R.-M. Wang), yuexin_liu@163.com (Y.-X. Liu), wanmengyuanwmy@163.com (M.-Y. Wan), huachongccc@163.com (C. Hua), jinhuanwuli@126.com (J.-H. Sheng), yuanguoxu@jxnu.edu.cn (Y.-G. Xu).

https://doi.org/10.1016/j.nuclphysb.2023.116349

1. Introduction

Semileptonic heavy meson decays dominated by tree-level exchange of W-bosons in the standard model have attracted a lot of attention in testing the standard model and in searching for the new physics beyond the standard model. Many semileptonic $D \to P/V\ell^+\nu_\ell$ decays and one $D \to S\ell^+\nu_\ell$ decay have been observed [1], present experimental measurements of the $D \to P/V\ell^+\nu_\ell$ decays give us an opportunity to additionally test theoretical approaches, and many $D \to S\ell^+\nu_\ell$ decays can be predicted by one measured $D \to S\ell^+\nu_\ell$ decay.

In theory, the description of semileptonic decays is relatively simple, and the weak and strong dynamics can be separated in these processes since leptons do not participate in the strong interaction. All the strong dynamics in the initial and final hadrons is included in the hadronic form factors, which are important for testing the theoretical calculations of the involved strong interaction. The form factors of the D decays have been calculated by many ways, for examples, quark model [2–7], QCD sum rules [8], light-cone sum rules [9–11], covariant light-front quark models [12–14], and lattice QCD [15,16]. Most studies of the form factors are focused on the $D \to P/V$ transitions, and less studies are focused on the $D \to S$ transitions.

The SU(3) flavor symmetry approach is independent of the detailed dynamics offering us an opportunity to relate different decay modes, nevertheless, it cannot determine the sizes of the amplitudes or the form factors by itself. However, if experimental data are enough, one may use the data to extract the amplitudes or the form factors, which can be viewed as predictions based on symmetry, has a smaller dependency on estimated form factors, and can provide some very useful information about the decays. The SU(3) flavor symmetry works well in the b-hadron decays [17–30], and the c-hadron decays [29–47].

Semileptonic decays of D mesons have been studied extensively in the standard model and its various extensions, for instance, in Refs. [3,48–59]. In this work, we will systematically study the $D \to P/V/S\ell^+\nu_\ell$ decays with the SU(3) flavor symmetry. We will firstly construct the amplitude relations between different decay modes of $D \to P\ell^+\nu_\ell$, $D \to V\ell^+\nu_\ell$ or $D \to S\ell^+\nu_\ell$ decays by the SU(3) flavor symmetry and the SU(3) flavor breaking. We use the available data to extract the SU(3) flavor symmetry/breaking amplitudes and the form factors, and then predict the not yet measured modes for further tests in experiments. The forward-backward asymmetries A_{FB}^ℓ, the lepton-side convexity parameters C_F^ℓ, the longitudinal polarizations of the final charged lepton P_L^ℓ, the transverse polarizations of the final charged lepton P_T^ℓ, the lepton spin asymmetries A_λ and the longitudinal polarization fractions F_L of the final vector mesons with two ways of integration have also been predicted in the $D \to P/V\ell^+\nu_\ell$ decays. In addition, the q^2 dependence of some differential observables for the $D \to P/V\ell^+\nu_\ell$ decays is shown in figures.

This paper will be organized as follows. In Sec. 2, the theoretical framework in this work is presented, including the effective hamiltonian, the hadronic helicity amplitude relations, the observables and the form factors. The numerical results of the $D \to P/V/S\ell^+\nu_\ell$ semileptonic decays will be given in Sec. 3. Finally, we give the summary and conclusion in Sec. 4.

2. Theoretical frame

2.1. The effective Hamiltonian

In the standard model, the four-fermion charged-current effective Hamiltonian below the electroweak scale for the decays $D \to M\ell^+\nu_\ell$ ($M = P, V, S$) can be written as

$$\mathcal{H}_{eff}(c \to q\ell^+\nu_\ell) = \frac{G_F}{\sqrt{2}} V_{cq}^* \bar{q}\gamma^\mu(1-\gamma_5)c\ \bar{\nu}_\ell\gamma_\mu(1-\gamma_5)\ell, \tag{1}$$

with $q = s, d$. The helicity amplitudes of the decays $D \to M\ell^+\nu_\ell$ can be written as

$$\mathcal{M}(D \to M\ell^+\nu_\ell) = \frac{G_F}{\sqrt{2}} \sum_{mm'} g_{mm'} L_m^{\lambda_\ell\lambda_\nu} H_{m'}^{\lambda_M}, \tag{2}$$

with

$$L_m^{\lambda_\ell\lambda_\nu} = \epsilon_\alpha(m)\bar{\nu}_\ell\gamma^\alpha(1-\gamma_5)\ell, \tag{3}$$

$$H_{\lambda_M m'}^M = \begin{cases} V_{cq}^*\epsilon_\beta^*(m')\langle P/S(p_{P/S})|\bar{q}\gamma^\beta(1-\gamma_5)c|D(p_D)\rangle \\ V_{cq}^*\epsilon_\beta^*(m')\langle V(p_V,\epsilon^*)|\bar{q}\gamma^\beta(1-\gamma_5)c|D(p_D)\rangle \end{cases}, \tag{4}$$

where the particle helicities $\lambda_M = 0$ for $M = P/S$, $\lambda_M = 0, \pm 1$ for $M = V$, $\lambda_\ell = \pm\frac{1}{2}$ and $\lambda_\nu = +\frac{1}{2}$, as well as $\epsilon_\mu(m)$ is the polarization vectors of the virtual W with $m = 0, t, \pm 1$. Note that the CKM matrix element V_{cq}^* is written into $H_{\lambda_M m'}^M$ for the later convenience.

The form factors of the $D \to P$, $D \to S$ and $D \to V$ transitions are given by [2,3,13]

$$\left\langle P(p)\left|\bar{d}_k\gamma_\mu c\right|D(p_D)\right\rangle = f_+^P(q^2)(p+p_D)_\mu + \left[f_0^P(q^2) - f_+^P(q^2)\right]\frac{m_D^2 - m_P^2}{q^2}q_\mu, \tag{5}$$

$$\left\langle S(p)\left|\bar{d}_k\gamma_\mu\gamma_5 c\right|D(p_D)\right\rangle = -i\left(f_+^S(q^2)(p+p_D)_\mu + \left[f_0^S(q^2) - f_+^S(q^2)\right]\frac{m_D^2 - m_S^2}{q^2}q_\mu\right), \tag{6}$$

$$\begin{aligned}\left\langle V(p,\varepsilon^*)\left|\bar{d}_k\gamma_\mu(1-\gamma_5)c\right|D(p_D)\right\rangle &= \frac{2V^V(q^2)}{m_D+m_V}\epsilon_{\mu\nu\alpha\beta}\varepsilon^{*\nu}p_D^\alpha p^\beta \\ &- i\left[\varepsilon_\mu^*(m_D+m_V)A_1^V(q^2) - (p_D+p)_\mu(\varepsilon^*.p_D)\frac{A_2^V(q^2)}{m_D+m_V}\right] \\ &+ iq_\mu(\varepsilon^*.p_D)\frac{2m_V}{q^2}[A_3^V(q^2) - A_0^V(q^2)],\end{aligned} \tag{7}$$

where $s = q^2$ ($q = p_D - p_M$), and ε^* is the polarization of vector meson. The hadronic helicity amplitudes can be written as

$$H_{\pm\pm}^P = 0, \tag{8}$$

$$H_{00}^P = \frac{2m_{D_q}|\vec{p}_P|}{\sqrt{q^2}}f_+^P(q^2)V_{cq}^*, \tag{9}$$

$$H_{0t}^P = \frac{m_{D_q}^2 - m_P^2}{\sqrt{q^2}}f_0^P(q^2)V_{cq}^*, \tag{10}$$

for $D \to P\ell^+\nu_\ell$ decays,

$$H_{\pm\pm}^S = 0, \tag{11}$$

$$H_{00}^S = \frac{i2m_{D_q}|\vec{p}_S|}{\sqrt{q^2}}f_+^S(q^2)V_{cq}^*, \tag{12}$$

$$H_{0t}^S = \frac{i(m_{D_q}^2 - m_S^2)}{\sqrt{q^2}}f_0^S(q^2)V_{cq}^*, \tag{13}$$

for $D \to S\ell^+\nu_\ell$ decays, and

$$H^V_{\pm\pm} = (m_{D_q} + m_V)A_1(q^2) \mp \frac{2m_{D_q}|\vec{p}_V|}{(m_{D_q}+m_V)}V(q^2)V^*_{cq}, \tag{14}$$

$$H^V_{00} = \frac{1}{2m_V\sqrt{q^2}}\left[(m^2_{D_q} - m^2_V - q^2)(m_{D_q}+m_V)A_1(q^2) - \frac{4m^2_{D_q}|\vec{p}_V|^2}{m_{D_q}+m_V}A_2(q^2)\right]V^*_{cq}, \tag{15}$$

$$H^V_{0t} = \frac{2m_{D_q}|\vec{p}_V|}{\sqrt{q^2}}A_0(q^2)V^*_{cq}, \tag{16}$$

for $D \to V\ell^+\nu_\ell$ decays, where $|\vec{p}_M| \equiv \sqrt{\lambda(m^2_{D_q}, m^2_M, q^2)}/2m_{D_q}$ with $\lambda(a,b,c) = a^2 + b^2 + c^2 - 2ab - 2ac - 2bc$.

2.2. Hadronic helicity amplitude relations by the SU(3) flavor symmetry

Charmed mesons containing one heavy c quark are flavor SU(3) anti-triplets

$$D_i = \left(D^0(c\bar{u}),\ D^+(c\bar{d}),\ D^+_s(c\bar{s})\right). \tag{17}$$

Light pseudoscalar P and vector V meson octets and singlets under the $SU(3)$ flavor symmetry of u, d, s quarks are [60]

$$P = \begin{pmatrix} \frac{\pi^0}{\sqrt{2}} + \frac{\eta_8}{\sqrt{6}} + \frac{\eta_1}{\sqrt{3}} & \pi^+ & K^+ \\ \pi^- & -\frac{\pi^0}{\sqrt{2}} + \frac{\eta_8}{\sqrt{6}} + \frac{\eta_1}{\sqrt{3}} & K^0 \\ K^- & \overline{K}^0 & -\frac{2\eta_8}{\sqrt{6}} + \frac{\eta_1}{\sqrt{3}} \end{pmatrix}, \tag{18}$$

$$V = \begin{pmatrix} \frac{\rho^0}{\sqrt{2}} + \frac{\omega_8}{\sqrt{6}} + \frac{\omega_1}{\sqrt{3}} & \rho^+ & K^{*+} \\ \rho^- & -\frac{\rho^0}{\sqrt{2}} + \frac{\omega_8}{\sqrt{6}} + \frac{\omega_1}{\sqrt{3}} & K^{*0} \\ K^{*-} & \overline{K}^{*0} & -\frac{2\omega_8}{\sqrt{6}} + \frac{\omega_1}{\sqrt{3}} \end{pmatrix}, \tag{19}$$

where ω and ϕ mix in an ideal form, and the η and η' (ω and ϕ) are mixtures of $\eta_1(\omega_1) = \frac{u\bar{u}+d\bar{d}+s\bar{s}}{\sqrt{3}}$ and $\eta_8(\omega_8) = \frac{u\bar{u}+d\bar{d}-2s\bar{s}}{\sqrt{6}}$ with the mixing angle θ_P (θ_V). η and η' (ω and ϕ) are given by

$$\begin{pmatrix} \eta \\ \eta' \end{pmatrix} = \begin{pmatrix} cos\theta_P & -sin\theta_P \\ sin\theta_P & cos\theta_P \end{pmatrix}\begin{pmatrix} \eta_8 \\ \eta_1 \end{pmatrix}, \qquad \begin{pmatrix} \phi \\ \omega \end{pmatrix} = \begin{pmatrix} cos\theta_V & -sin\theta_V \\ sin\theta_V & cos\theta_V \end{pmatrix}\begin{pmatrix} \omega_8 \\ \omega_1 \end{pmatrix}, \tag{20}$$

where $\theta_P = [-20^\circ, -10^\circ]$ and $\theta_V = 36.4^\circ$ from Particle Data Group (PDG) [1] will be used in our numerical analysis.

The structures of the light scalar mesons are not fully understood yet. Many suggestions are discussed, such as ordinary two quark states, four quark states, meson-meson bound states, molecular states, glueball states or hybrid states, for examples, in Refs. [61–69]. In this work, we will consider the two quark and the four quark scenarios for the scalar mesons below or near 1 GeV. In the two quark picture, the light scalar mesons can be written as [70]

$$S=\begin{pmatrix} \frac{a_0^0}{\sqrt{2}}+\frac{\sigma}{\sqrt{2}} & a_0^+ & K_0^+ \\ a_0^- & -\frac{a_0^0}{\sqrt{2}}+\frac{\sigma}{\sqrt{2}} & K_0^0 \\ K_0^- & \overline{K}_0^0 & f_0 \end{pmatrix}. \tag{21}$$

The two isoscalars $f_0(980)$ and $f_0(500)$ are obtained by the mixing of $\sigma=\frac{u\bar{u}+d\bar{d}}{\sqrt{2}}$ and $f_0=s\bar{s}$

$$\begin{pmatrix} f_0(980) \\ f_0(500) \end{pmatrix}=\begin{pmatrix} \cos\theta_S & \sin\theta_S \\ -\sin\theta_S & \cos\theta_S \end{pmatrix}\begin{pmatrix} f_0 \\ \sigma \end{pmatrix}, \tag{22}$$

where the three possible ranges of the mixing angle, $25^\circ<\theta_S<40^\circ$, $140^\circ<\theta_S<165^\circ$ and $-30^\circ<\theta_S<30^\circ$ [61,71] will be analyzed in our numerical results. In the four quark picture, the light scalar mesons are given as [1,72]

$$\begin{aligned} &\sigma=u\bar{u}d\bar{d}, && f_0=(u\bar{u}+d\bar{d})s\bar{s}/\sqrt{2}, \\ &a_0^0=(u\bar{u}-d\bar{d})s\bar{s}/\sqrt{2}, && a_0^+=ud\bar{s}\bar{s}, && a_0^-=d\bar{u}s\bar{s}, \\ &K_0^+=us\bar{d}\bar{d}, && K_0^0=d\bar{s}u\bar{u}, && \bar{K}_0^0=s\bar{d}u\bar{u}, && K_0^-=s\bar{u}d\bar{d}, \end{aligned} \tag{23}$$

which are noted by S^{im}_{jm}. The two isoscalars are expressed as

$$\begin{pmatrix} f_0(980) \\ f_0(500) \end{pmatrix}=\begin{pmatrix} \cos\phi_S & \sin\phi_S \\ -\sin\phi_S & \cos\phi_S \end{pmatrix}\begin{pmatrix} f_0 \\ \sigma \end{pmatrix}, \tag{24}$$

where the constrained mixing angle $\phi_S=(174.6^{+3.4}_{-3.2})^\circ$ [62].

In terms of the SU(3) flavor symmetry, meson states and quark operators can be parameterized into SU(3) tensor forms, while the leptonic helicity amplitudes $L_m^{\lambda_\ell,\lambda_\nu}$ are invariant under the SU(3) flavor symmetry. And the hadronic helicity amplitude relations of the $D\to M\ell^+\nu_\ell(M=P,V,S)$ decays can be parameterized as

$$H^M_{\lambda_M m'}(D\to M\ell^+\nu_\ell)=c_0^M D_i M^i_j H^j, \tag{25}$$

where $H^2\equiv V_{cd}^*$ and $H^3\equiv V_{cs}^*$ are the CKM matrix elements, c_0^M are the nonperturbative coefficients of the $D\to M\ell^+\nu_\ell$ decays under the SU(3) flavor symmetry, and we use that $c_i^M\equiv c_{i\ \lambda_M m'}^M$ and $c_i'^M\equiv c_{i\ \lambda_M m'}'^M$ in this paper. Note that the hadronic helicity amplitudes for the $D\to S\ell^+\nu_\ell$ decays in Eq. (25) are given in the two quark picture of the light scalar mesons, and ones in the four quark picture of the light scalar mesons will be given later.

The SU(3) flavor breaking effects mainly come from different masses of u, d and s quarks, and they have been analyzed in many works, for examples, in Refs. [73–79]. The diagonalized mass matrix can be expressed as [78,79]

$$\begin{pmatrix} m_u & 0 & 0 \\ 0 & m_d & 0 \\ 0 & 0 & m_s \end{pmatrix}=\frac{1}{3}(m_u+m_d+m_s)I+\frac{1}{2}(m_u-m_d)X+\frac{1}{6}(m_u+m_d-2m_s)W, \tag{26}$$

with

$$X=\begin{pmatrix} 1 & 0 & 0 \\ 0 & -1 & 0 \\ 0 & 0 & 0 \end{pmatrix}, \qquad W=\begin{pmatrix} 1 & 0 & 0 \\ 0 & 1 & 0 \\ 0 & 0 & -2 \end{pmatrix}. \tag{27}$$

Compared with s quark mass, the u and d quark masses are much smaller which can be ignored. The SU(3) flavor breaking effects due to a non-zero s quark mass dominate the SU(3) breaking effects. When u and d quark mass difference is ignored, the residual SU(3) flavor symmetry becomes the isospin symmetry and the term proportional to X can be dropped. The identity I part contributes to the $D \to M\ell^+\nu_\ell$ decay amplitudes in a similar way as that given in Eq. (25) which can be absorbed into the coefficients c_0^M. Only W part will contribute to the SU(3) breaking effects. The SU(3) breaking amplitudes of the $D \to M\ell^+\nu_\ell$ decays can be given as

$$\Delta H^M_{\lambda_M m'}(D \to M\ell^+\nu_\ell) = c_1^M D_a W_i^a M_j^i H^j + c_2^M D_i M_a^i W_j^a H^j, \tag{28}$$

where $c_{1,2}^M$ are the nonperturbative SU(3) flavor breaking coefficients.

In the four quark picture of the light scalar mesons, the hadronic helicity amplitudes of the $D \to S\ell^+\nu_\ell$ decays under the SU(3) flavor symmetry are

$$H^{S,4q}_{\lambda_M m'}(D \to S\ell^+\nu_\ell) = c_0'^S D_i S_{jm}^{im} H^j, \tag{29}$$

and the corresponding SU(3) flavor breaking amplitudes of the $D \to S\ell^+\nu_\ell$ decays are

$$\Delta H^{S,4q}_{\lambda_M m'}(D \to S\ell^+\nu_\ell) = c_1'^S D_a W_i^a S_{jm}^{im} H^j + c_2'^S D_i S_{am}^{im} W_j^a H^j + c_3'^S D_i S_{ja}^{im} W_m^a H^j, \tag{30}$$

here $c_{0,1,2,3}'^S$ are the nonperturbative coefficients.

In terms of the SU(3) flavor symmetry, the hadronic helicity amplitude relations for the $D \to P\ell^+\nu_\ell$, $D \to V\ell^+\nu_\ell$ and $D \to S\ell^+\nu_\ell$ decays are summarized in later Table 1, Table 4 and Table 8, respectively.

2.3. Observables for the $D \to M\ell^+\nu_\ell$ decays

The double differential branching ratios of the $D \to M\ell^+\nu_\ell$ decays are [59]

$$\begin{aligned}\frac{d\mathcal{B}(D \to M\ell^+\nu_\ell)}{dq^2 d(\cos\theta)} = &\frac{\tau_D G_F^2 |V_{cq}|^2 \lambda^{1/2}(q^2 - m_\ell^2)^2}{64(2\pi)^3 M_{D_{(s)}}^3 q^2} \\ &\times \Big[(1+\cos^2\theta)\mathcal{H}_U + 2\sin^2\theta\mathcal{H}_L + 2\cos\theta\mathcal{H}_P \\ &+ \frac{m_\ell^2}{q^2}(\sin^2\theta\mathcal{H}_U + 2\cos^2\theta\mathcal{H}_L + 2\mathcal{H}_S - 4\cos\theta\mathcal{H}_{SL})\Big],\end{aligned} \tag{31}$$

where $\lambda \equiv \lambda(m_{D_q}^2, m_M^2, q^2)$, $m_\ell^2 \le q^2 \le (m_{D_q} - m_M)^2$, and

$$\begin{aligned}&\mathcal{H}_U = |H_{++}^M|^2 + |H_{--}^M|^2, \quad \mathcal{H}_L = |H_{00}^M|^2, \quad \mathcal{H}_P = |H_{++}^M|^2 - |H_{--}^M|^2, \\ &\mathcal{H}_S = |H_{0t}^M|^2, \quad \mathcal{H}_{SL} = \Re(H_{00}^M H_{0t}^{M\dagger}).\end{aligned} \tag{32}$$

The differential branching ratios integrated over $\cos\theta$ are [59]

$$\frac{d\mathcal{B}(D_{(s)} \to M\ell^+\nu_\ell)}{dq^2} = \frac{\tau_D G_F^2 |V_{cq}|^2 \lambda^{1/2}(q^2 - m_\ell^2)^2}{24(2\pi)^3 M_{D_{(s)}}^3 q^2}\mathcal{H}_{\text{total}}, \tag{33}$$

with

$$\mathcal{H}_{\text{total}} \equiv (\mathcal{H}_U + \mathcal{H}_L)\left(1 + \frac{m_\ell^2}{2q^2}\right) + \frac{3m_\ell^2}{2q^2}\mathcal{H}_S. \tag{34}$$

The forward-backward asymmetries are defined as [59]

$$A_{FB}^{\ell}(q^2) = \frac{\int_{-1}^{0} d\cos\theta_\ell \frac{d\mathcal{B}(D\to M\ell\nu)}{dq^2 d\cos\theta_\ell} - \int_{0}^{1} d\cos\theta_\ell \frac{d\mathcal{B}(D\to M\ell\nu)}{dq^2 d\cos\theta_\ell}}{\int_{-1}^{0} d\cos\theta_\ell \frac{d\mathcal{B}(D\to M\ell\nu)}{dq^2 d\cos\theta_\ell} + \int_{0}^{1} d\cos\theta_\ell \frac{d\mathcal{B}(D\to M\ell\nu)}{dq^2 d\cos\theta_\ell}} \tag{35}$$

$$= \frac{3}{4}\frac{\mathcal{H}_P - \frac{2m_\ell^2}{q^2}\mathcal{H}_{SL}}{\mathcal{H}_{\rm total}}. \tag{36}$$

The lepton-side convexity parameters are given by [59]

$$C_F^{\ell}(q^2) = \frac{3}{4}\left(1 - \frac{m_\ell^2}{q^2}\right)\frac{\mathcal{H}_U - 2\mathcal{H}_L}{\mathcal{H}_{\rm total}}. \tag{37}$$

The longitudinal polarizations of the final charged lepton ℓ are defined by [59]

$$P_L^{\ell}(q^2) = \frac{(\mathcal{H}_U + \mathcal{H}_L)\left(1 - \frac{m_\ell^2}{2q^2}\right) - \frac{3m_\ell^2}{2q^2}\mathcal{H}_S}{\mathcal{H}_{\rm total}}, \tag{38}$$

and its transverse polarizations are

$$P_T^{\ell}(q^2) = -\frac{3\pi m_\ell}{8\sqrt{q^2}}\frac{\mathcal{H}_P + 2\mathcal{H}_{SL}}{\mathcal{H}_{\rm total}}. \tag{39}$$

The lepton spin asymmetries in the $\ell - \bar{\nu}_\ell$ center of mass frame are defined by [80–83]

$$A_\lambda(q^2) = \frac{d\mathcal{B}(D\to M\ell^+\nu_\ell)[\lambda_\ell = -\frac{1}{2}]/dq^2 - d\mathcal{B}(D\to M\ell^+\nu_\ell)[\lambda_\ell = +\frac{1}{2}]/dq^2}{d\mathcal{B}(D\to M\ell^+\nu_\ell)[\lambda_\ell = -\frac{1}{2}]/dq^2 + d\mathcal{B}(D\to M\ell^+\nu_\ell)[\lambda_\ell = +\frac{1}{2}]/dq^2} \tag{40}$$

$$= \frac{\mathcal{H}_{\rm total} - \frac{6m_\ell^2}{2q^2}\mathcal{H}_{\rm S}}{\mathcal{H}_{\rm total}}. \tag{41}$$

For the $D \to V\ell^+\nu_\ell$ decays, the longitudinal polarization fractions of the final vector mesons are given by [59]

$$F_L(q^2) = \frac{\mathcal{H}_L\left(1 + \frac{m_\ell^2}{2q^2}\right) + \frac{3m_\ell^2}{2q^2}\mathcal{H}_S}{\mathcal{H}_{\rm total}}, \tag{42}$$

then its transverse polarization fractions $F_T(q^2) = 1 - F_L(q^2)$.

Note that, for q^2-integration of $X(q^2) = A_{FB}^{\ell},\ C_F^{\ell},\ P_L^{\ell},\ P_T^{\ell},\ A_\lambda$ and F_L, following Ref. [84], two ways of integration are considered. The normalized q^2-integrated observables $\langle X\rangle$ are calculated by separately integrating the numerators and denominators with the same q^2 bins. The "naively integrated" observables are obtained by

$$\overline{X} = \frac{1}{q^2_{max} - q^2_{min}}\int_{q^2_{min}}^{q^2_{max}} dq^2 X(q^2). \tag{43}$$

2.4. Form factors

In order to obtain more precise observables, one also needs consider the q^2 dependence of the form factors for the $D \to P\ell^+\nu_\ell$, $D \to V\ell^+\nu_\ell$ and $D \to S\ell^+\nu_\ell$ decays. The following cases will be considered in our analysis of $D \to P/V\ell^+\nu_\ell$ decays.

C_1: All form factors are treated as constants without the hadronic momentum-transfer q^2 dependence, and different form factors are related by the SU(3) flavor symmetry, *i.e.*, the SU(3) flavor breaking terms such as $c^M_{1,2}$ and $c'^S_{1,2,3}$ in later Tables 1, 4 and 8 are ignored.

C_2: With the SU(3) flavor symmetry, the modified pole model for the q^2-dependence of $F_i(q^2)$ is used [85]

$$F_i(q^2) = \frac{F_i(0)}{\left(1-\frac{q^2}{m^2_{pole}}\right)\left(1-\alpha_i\frac{q^4}{m^4_{pole}}\right)}, \tag{44}$$

where $m_{pole} = m_{D^{*+}}$ for $c \to d\ell^+\nu_\ell$ transitions and $m_{pole} = m_{D_s^{*+}}$ for $c \to s\ell^+\nu_\ell$ transitions, and α_i are free parameters and are different for $f_+^P(q^2)$, $f_0^P(q^2)$, $V(q^2)$, $A_1(q^2)$ and $A_2(q^2)$, we will take $\alpha_i \in [-1, 1]$ in our analysis.

C_3: With the SU(3) flavor symmetry, following Ref. [2]

$$F_i(q^2) = \frac{F_i(0)}{\left(1-\frac{q^2}{m^2_{pole}}\right)\left(1-\sigma_{1i}\frac{q^2}{m^2_{pole}}+\sigma_{2i}\frac{q^4}{m^4_{pole}}\right)} \quad \text{for } f_+^P(q^2) \text{ and } V(q^2), \tag{45}$$

$$F_i(q^2) = \frac{F_i(0)}{\left(1-\sigma_{1i}\frac{q^2}{m^2_{pole}}+\sigma_{2i}\frac{q^4}{m^4_{pole}}\right)} \quad \text{for } f_0^P(q^2), A_1(q^2) \text{ and } A_2(q^2), \tag{46}$$

where $\sigma_{1,2}$ for the $D \to \pi$ and $D \to K^*$ transitions from Ref. [2] will be used in our results.

C_4: Considering the SU(3) flavor breaking terms such as $c^M_{1,2}$ and $c'^S_{1,2,3}$ in later Tables 1, 4 and 8, the form factors in C_3 case are used.

As for the form factors of the $D \to S\ell^+\nu_\ell$ decays, we find that the vector dominance model [86] and the double pole model [87] give the similar SU(3) flavor symmetry predictions for the branching ratios of the $D \to S\ell^+\nu_\ell$ decays. The following form factors from the vector dominance model will be used in the numerical results,

$$F_i(q^2) = \frac{F_i(0)}{\left(1-q^2/m^2_{pole}\right)} \quad \text{for } f_+^S(q^2) \text{ and } f_0^S(q^2). \tag{47}$$

After considering above q^2 dependence, we only need to focus on the $F_i(0)$. Since these form factors $F_i(0)$ also preserve the SU(3) flavor symmetry, the same relations in Tables 1, 4 and 8 will be used for $F_i(0)$. If considering the form factors ratios $f_+(0)/f_0(0) = 1$ for $D \to P/S\ell^+\nu_\ell$ decays, $r_V \equiv V(0)/A_1(0) = 1.46 \pm 0.07$, $r_2 \equiv A_2(0)/A_1(0) = 0.68 \pm 0.06$ in $D^0 \to K^{*-}\ell^+\nu_\ell$ decays from PDG [1] and the SU(3) flavor symmetry, there is only one free form factor $f_+^{P,S}(0)$ and $A_1(0)$ for the $D \to P/S\ell^+\nu_\ell$ and $D \to V\ell^+\nu_\ell$ decays, respectively. As a result, the branching ratios only depend on one form factor $f_+^P(0)$, $f_+^S(0)$ or $A_1(0)$ and the CKM matrix element V_{cq}.

Table 1
The hadronic helicity amplitudes for the $D \to P\ell^+\nu$ decays including both the SU(3) flavor symmetry and the SU(3) flavor breaking contributions. $A_1 \equiv c_0^P + c_1^P - 2c_2^P$, $A_2 \equiv c_0^P - 2c_1^P - 2c_2^P$, $A_3 \equiv c_0^P + c_1^P + c_2^P$, $A_4 \equiv c_0^P - 2c_1^P + c_2^P$. $A_1 = A_2 = A_3 = A_4 = c_0^P$ if neglecting the SU(3) flavor breaking c_1^P and c_2^P terms.

Hadronic helicity amplitudes	SU(3) flavor amplitudes
$H(D^0 \to K^-\ell^+\nu_\ell)$	$A_1 V_{cs}^*$
$H(D^+ \to \overline{K}^0\ell^+\nu_\ell)$	$A_1 V_{cs}^*$
$H(D_s^+ \to \eta\ell^+\nu_\ell)$	$\big(-cos\theta_P\sqrt{2/3} - sin\theta_P/\sqrt{3}\big)A_2 V_{cs}^*$
$H(D_s^+ \to \eta'\ell^+\nu_\ell)$	$\big(-sin\theta_P\sqrt{2/3} + cos\theta_P/\sqrt{3}\big)A_2 V_{cs}^*$
$H(D_s^+ \to \pi^0\ell^+\nu_\ell)$	$-\delta\big(-cos\theta_P\sqrt{2/3} - sin\theta_P/\sqrt{3}\big)A_2 V_{cs}^*$
$H(D^0 \to \pi^-\ell^+\nu_\ell)$	$A_3 V_{cd}^*$
$H(D^+ \to \pi^0\ell^+\nu_\ell)$	$-\frac{1}{\sqrt{2}}A_3 V_{cd}^*$
$H(D^+ \to \eta\ell^+\nu_\ell)$	$\big(cos\theta_P/\sqrt{6} - sin\theta_P/\sqrt{3}\big)A_3 V_{cd}^*$
$H(D^+ \to \eta'\ell^+\nu_\ell)$	$\big(sin\theta_P/\sqrt{6} + cos\theta_P/\sqrt{3}\big)A_3 V_{cd}^*$
$H(D_s^+ \to K^0\ell^+\nu_\ell)$	$A_4 V_{cd}^*$

3. Numerical results

The theoretical input parameters and the experimental data within the 2σ errors from PDG [1] will be used in our numerical results.

3.1. $D \to P\ell^+\nu_\ell$ decays

Considering both the SU(3) flavor symmetry and the SU(3) flavor breaking contributions, the hadronic helicity amplitudes for the $D \to P\ell^+\nu_\ell$ decays are given in Table 1, in which we keep the CKM matrix element V_{cs} and V_{cd} information for comparing conveniently. In addition, $H(D_s^+ \to \pi^0\ell^+\nu_\ell)$ are obtained by neutral meson mixing with $\delta^2 = (5.18 \pm 0.71) \times 10^{-4}$ in Ref. [85]. From Table 1, we can easily see the hadronic helicity amplitude relations of the $D \to P\ell^+\nu_\ell$ decays. There are four nonperturbative parameters $A_{1,2,3,4}$ in the $D \to P\ell^+\nu_\ell$ decays with $A_1 \equiv c_0^P + c_1^P - 2c_2^P$, $A_2 \equiv c_0^P - 2c_1^P - 2c_2^P$, $A_3 \equiv c_0^P + c_1^P + c_2^P$ and $A_4 \equiv c_0^P - 2c_1^P + c_2^P$. If neglecting the SU(3) flavor breaking c_1^P and c_2^P terms, $A_1 = A_2 = A_3 = A_4 = c_0^P$, and then all hadronic helicity amplitudes are related by only one parameter c_0^P.

Many decay modes of the $D \to Pe^+\nu_e$, $P\mu^+\nu_\mu$ decays have been measured, and the experimental data with 2σ errors are listed in the second column of Table 2. One can constrain the parameters A_i or $f_+^P(0)$ by the present experimental data within 2σ errors and then predict other not yet measured branching ratios. Four cases $C_{1,2,3,4}$ will be considered in our analysis. The constrained form factor $f_+^P(0)$ is 0.876 ± 0.003, 0.763 ± 0.097 and 0.737 ± 0.003 in the C_1, C_2 and C_3 cases, respectively. The numerical results of $\mathcal{B}(D \to P\ell^+\nu_\ell)$ in the C_1, C_2, C_3 and C_4 cases are given in the third, fourth, fifth and sixth columns of Table 2, respectively. And our comments on the results are as follows.

- **Results in C_1 case:** From the third column of Table 2, one can see that the SU(3) flavor symmetry predictions of $\mathcal{B}(D \to P\ell^+\nu_\ell)$ in the C_1 case are entirely consistent with all present experiential data. The not yet measured branching ratios of the $D_s^+ \to \pi^0 e^+\nu_e$, $D_s^+ \to \pi^0\mu^+\nu_\mu$, $D^+ \to \eta'\mu^+\nu_\mu$ and $D_s^+ \to K^0\mu^+\nu_\mu$ decays are predicted on the order

Table 2
Branching ratios of the $D \to P\ell^+\nu$ decays. †Denotes that the corresponding experimental data from PDG [1] are not used to constrain A_i in this case.

Branching ratios	Exp. data	Ones in C_1	Ones in C_2	Ones in C_3	Ones in C_4	Previous ones
$\mathcal{B}(D^+ \to \overline{K}^0 e^+\nu_e)(\times 10^{-2})$	8.72 ± 0.18	8.84 ± 0.06	8.83 ± 0.07	8.84 ± 0.06	8.83 ± 0.07	
$\mathcal{B}(D^+ \to \pi^0 e^+\nu_e)(\times 10^{-3})$	3.72 ± 0.34	3.75 ± 0.05	$5.40 \pm 1.33^\dagger$	$5.04 \pm 0.12^\dagger$	3.70 ± 0.11	
$\mathcal{B}(D^+ \to \eta e^+\nu_e)(\times 10^{-3})$	1.11 ± 0.14	1.15 ± 0.05	1.20 ± 0.05	1.20 ± 0.05	0.92 ± 0.08	
$\mathcal{B}(D^+ \to \eta' e^+\nu_e)(\times 10^{-4})$	2.0 ± 0.8	2.59 ± 0.14	2.22 ± 0.34	2.09 ± 0.14	1.50 ± 0.20	
$\mathcal{B}(D^0 \to K^- e^+\nu_e)(\times 10^{-2})$	3.549 ± 0.052	3.52 ± 0.02	3.52 ± 0.03	3.52 ± 0.03	3.52 ± 0.02	
$\mathcal{B}(D^0 \to \pi^- e^+\nu_e)(\times 10^{-3})$	2.91 ± 0.08	2.95 ± 0.03	$4.23 \pm 1.03^\dagger$	$3.97 \pm 0.09^\dagger$	2.89 ± 0.06	
$\mathcal{B}(D_s^+ \to \eta e^+\nu_e)(\times 10^{-2})$	2.32 ± 0.16	2.37 ± 0.11	2.34 ± 0.14	2.36 ± 0.12	2.32 ± 0.16	
$\mathcal{B}(D_s^+ \to \eta' e^+\nu_e)(\times 10^{-3})$	8.0 ± 1.4	9.05 ± 0.04	8.25 ± 1.13	8.04 ± 0.43	8.02 ± 1.38	
$\mathcal{B}(D_s^+ \to K^0 e^+\nu_e)(\times 10^{-3})$	3.4 ± 0.8	3.10 ± 0.08	3.56 ± 0.39	3.54 ± 0.12	3.40 ± 0.80	
$\mathcal{B}(D_s^+ \to \pi^0 e^+\nu_e)(\times 10^{-5})$	···	1.51 ± 0.07	2.10 ± 0.56	1.96 ± 0.10	1.92 ± 0.13	2.65 ± 0.38 [85]
$\mathcal{B}(D^+ \to \overline{K}^0 \mu^+\nu_\mu)(\times 10^{-2})$	8.76 ± 0.38	8.56 ± 0.06	8.69 ± 0.15	8.61 ± 0.06	8.61 ± 0.06	
$\mathcal{B}(D^+ \to \pi^0 \mu^+\nu_\mu)(\times 10^{-3})$	3.50 ± 0.30	3.67 ± 0.05	$5.32 \pm 1.31^\dagger$	$4.96 \pm 0.12^\dagger$	3.64 ± 0.10	
$\mathcal{B}(D^+ \to \eta \mu^+\nu_\mu)(\times 10^{-3})$	1.04 ± 0.22	1.11 ± 0.05	1.18 ± 0.07	1.17 ± 0.05	0.90 ± 0.08	1.21 [7] 0.75 ± 0.15 [88]
$\mathcal{B}(D^+ \to \eta' \mu^+\nu_\mu)(\times 10^{-4})$	···	2.42 ± 0.13	2.10 ± 0.33	1.96 ± 0.13	1.41 ± 0.19	2.11 [7] 1.06 ± 0.20 [88]
$\mathcal{B}(D^0 \to K^- \mu^+\nu_\mu)(\times 10^{-2})$	3.41 ± 0.08	3.41 ± 0.02	3.44 ± 0.05	3.43 ± 0.02	3.43 ± 0.02	
$\mathcal{B}(D^0 \to \pi^- \mu^+\nu_\mu)(\times 10^{-3})$	2.67 ± 0.24	2.89 ± 0.02	$4.17 \pm 1.01^\dagger$	$3.90 \pm 0.09^\dagger$	2.85 ± 0.06	
$\mathcal{B}(D_s^+ \to \eta \mu^+\nu_\mu)(\times 10^{-2})$	2.4 ± 1.0	2.30 ± 0.10	2.30 ± 0.17	2.31 ± 0.12	2.26 ± 0.16	
$\mathcal{B}(D_s^+ \to \eta' \mu^+\nu_\mu)(\times 10^{-2})$	1.1 ± 1.0	0.86 ± 0.03	0.79 ± 0.11	0.77 ± 0.04	0.76 ± 0.13	
$\mathcal{B}(D_s^+ \to K^0 \mu^+\nu_\mu)(\times 10^{-3})$	···	3.01 ± 0.08	3.51 ± 0.38	3.46 ± 0.11	3.33 ± 0.78	3.9 [7] 3.85 ± 0.76 [88]
$\mathcal{B}(D_s^+ \to \pi^0 \mu^+\nu_\mu)(\times 10^{-5})$	···	1.48 ± 0.07	2.09 ± 0.53	1.93 ± 0.10	1.89 ± 0.13	
$\mathcal{B}(D_s^+ \to \pi^0 \tau^+\nu_\tau)(\times 10^{-10})$	···	3.45 ± 0.21	160.34 ± 149.53	4.20 ± 0.26	4.08 ± 0.34	$(27 \sim 36)$ [85]

of $\mathcal{O}(10^{-3} - 10^{-5})$, nevertheless, $\mathcal{B}(D_s^+ \to \pi^0\tau^+\nu_\tau)$ is predicted on the order of $\mathcal{O}(10^{-10})$ due to its narrow phase space and $(q^2 - m_\tau^2)^2$ suppression of the differential branching ratios in Eq. (33).

- **Results in $C_{2,3}$ cases:** The numerical results in $C_{2,3}$ cases are similar. The experimental upper limits of $\mathcal{B}(D^+ \to \pi^0\ell^+\nu_\ell)$ and $\mathcal{B}(D^0 \to \pi^-\ell^+\nu_\ell)$ have not been used to constrain the predictions of $\mathcal{B}(D \to P\ell^+\nu_\ell)$, since the upper limits of the predictions of $\mathcal{B}(D^+ \to \pi^0\ell^+\nu_\ell)$ and $\mathcal{B}(D^0 \to \pi^-\ell^+\nu_\ell)$ by the SU(3) flavor symmetry in $C_{2,3}$ cases are slightly larger than their experimental data. Other SU(3) flavor symmetry predictions are consistent with their experimental data within 2σ errors.
- **Results in C_4 case:** As given in the sixth column of Table 2, if considering both the hadronic momentum-transfer q^2 dependence of the form factors and the SU(3) flavor breaking contributions, all SU(3) flavor symmetry predictions are consistent with their experimental data within 2σ errors. For some decays, the errors of the theoretical predictions are much smaller than ones of their experimental data.
- The previous predictions for the not yet measured branching ratios are listed in the last column of Table 2, our predictions are in the same order of magnitude as previous ones for the $D \to Pe^+\nu_e, P\mu^+\nu_\mu$ decays. Even if our expression of $\mathcal{B}(D \to P\ell^+\nu_\ell)$ is identical to one in Ref. [85], our predictions of $\mathcal{B}(D_s^+ \to \pi^0\tau^+\nu_\tau)$ are quite different from one in Ref. [85]. Unlike $\mathcal{B}(D_s^+ \to \pi^0 e^+\nu_e)$ and $\mathcal{B}(D_s^+ \to \pi^0\mu^+\nu_\mu)$, since the term related to $|f_+^P(q^2)|^2$ is suppressed by $|\vec{p}_P|^2$ in $\mathcal{B}(D_s^+ \to \pi^0\tau^+\nu_\tau)$, the dominant contribution of

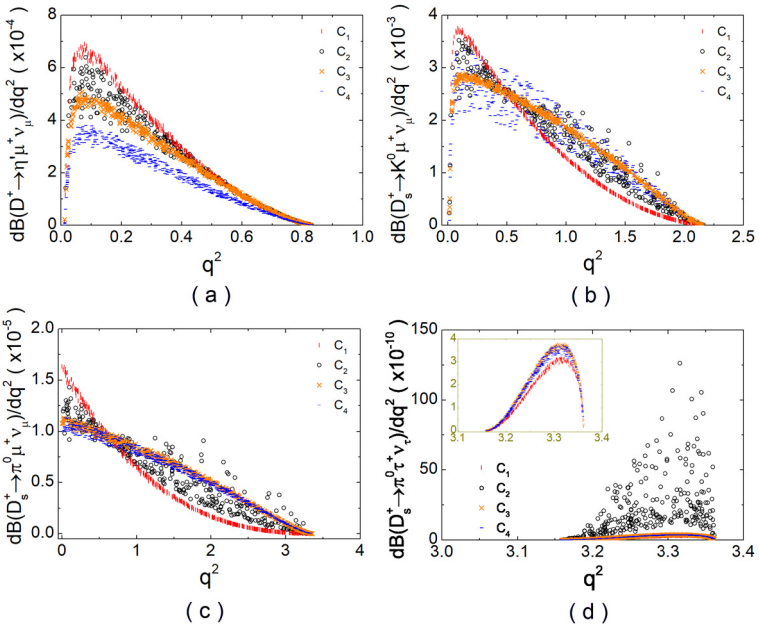

Fig. 1. The q^2 dependence of the differential branching ratios for some $D \to P\ell^+\nu_\ell$ with present experimental bounds.

$\mathcal{B}(D_s^+ \to \pi^0\tau^+\nu_\tau)$ comes from the term related to $|f_0^P(q^2)|^2$. The difference between our predictions of $\mathcal{B}(D_s^+ \to \pi^0\tau^+\nu_\tau)$ and one in Ref. [85] mainly comes from the choice of the form factors. Note that $\mathcal{B}(D_s^+ \to \pi^0\tau^+\nu_\tau)$ is predicted with quite large error in C_2 case in this work, which is due to our free parameter $\alpha_{f_0^P(q^2)} \in [-1, 1]$ in the form factor $f_0^P(q^2)$.

For the q^2 dependence of the differential branching ratios of the $D \to P\ell^+\nu_\ell$ decays with present experimental bounds, we only show the not yet measured processes $D^+ \to \eta'\mu^+\nu_\mu$, $D_s^+ \to K^0\mu^+\nu_\mu$, $D_s^+ \to \pi^0\mu^+\nu_\mu$ and $D_s^+ \to \pi^0\tau^+\nu_\tau$ in Fig. 1. We do not show $d\mathcal{B}(D_s^+ \to \pi^0 e^+\nu_e)/dq^2$, since it is similar to $d\mathcal{B}(D_s^+ \to \pi^0\mu^+\nu_\mu)/dq^2$ in Fig. 1 (c). From Fig. 1, one can see that present experimental measurements give quite strong bounds on the differential branching ratios of $D^+ \to \eta'\mu^+\nu_\mu$, $D_s^+ \to \pi^0\mu^+\nu_\mu$ and $D_s^+ \to \pi^0\tau^+\nu_\tau$ decays in the C_1, C_3 and C_4 cases as well as $D_s^+ \to K^0\mu^+\nu_\mu$ decays in the C_1 and C_3 cases, and all predictions of the four differential branching ratios in the C_2 case have a large error due to the form factor choice. Comparing with $d\mathcal{B}(D_s^+ \to \pi^0\mu^+\nu_\mu)/dq^2$ in Fig. 1 (c), as shown in Fig. 1 (d), $d\mathcal{B}(D_s^+ \to \pi^0\tau^+\nu_\tau)/dq^2$ is suppressed about the order of $\mathcal{O}(10^{-4})$ by $(q^2 - m_\tau^2)^2$.

The forward-backward asymmetries A_{FB}^ℓ, the lepton-side convexity parameters C_F^ℓ, the longitudinal polarizations of the final charged leptons P_L^ℓ and the transverse polarizations of the final charged leptons P_T^ℓ with two ways of integration for the $D \to P\ell^+\nu_\ell$ decays could also be obtained. These predictions are very accurate, and they are similar to each other in the four $C_{1,2,3,4}$ cases. So we only give the predictions within the C_3 case in Table 3 for examples. From Table 3, one can see that the predictions are obviously different between two ways of q^2 integration, and the slight difference in the same way of q^2 integration is due to the different decay phase spaces. For displaying the differences between the $D \to Pe^+\nu_e$ and $D \to P\mu^+\nu_\mu$ decays, we take $D_s^+ \to K^0 e^+\nu_e$ and $D_s^+ \to K^0\mu^+\nu_\mu$ as examples. The differential forward-backward

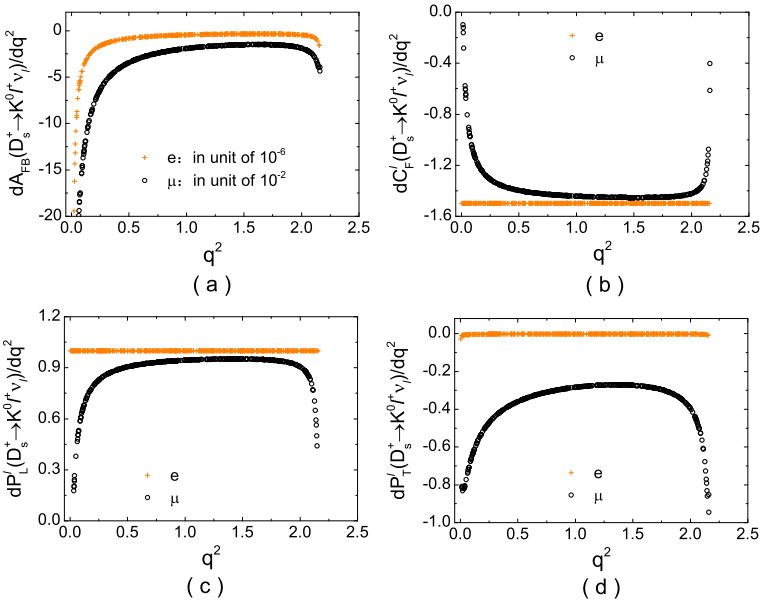

Fig. 2. The differential forward-backward asymmetries, differential lepton-side convexity parameters, differential longitudinal lepton polarizations and differential transverse lepton polarizations for the $D_s^+ \to K^0\ell^+\nu_\ell$ decays in the C_3 case.

asymmetries, the differential lepton-side convexity parameters, the differential longitudinal lepton polarizations and the differential transverse lepton polarizations of $D_s^+ \to K^0 e^+\nu_e$ and $D_s^+ \to K^0\mu^+\nu_\mu$ decays within the C_3 case are displayed in Fig. 2. And one can see that differential observables between $\ell = e$ and $\ell = \mu$ are obviously different, specially in the low and high q^2 ranges. As given an example of $dA_{FB}^{\ell}(D_s^+ \to K^0\ell^+\nu_\ell)/dq^2$ in Fig. 2 (a), all $dA_{FB}^{\ell}(D \to P\ell^+\nu_\ell)/dq^2$ are proportional to m_ℓ^2, so they are very small when $\ell = e$ and $\ell = \mu$, and $\frac{dA_{FB}^{\ell}(D\to Pe^+\nu_e)}{dq^2} : \frac{dA_{FB}^{\ell}(D\to P\mu^+\nu_\mu)}{dq^2} \sim m_e^2 : m_\mu^2 \approx 2.3 \times 10^{-5}$.

3.2. $D \to V\ell^+\nu_\ell$ decays

The hadronic helicity amplitudes for the $D \to V\ell^+\nu_\ell$ decays are given in Table 4. There are four nonperturbative parameters $B_{1,2,3,4}$ in the $D \to V\ell^+\nu_\ell$ decay modes. If neglecting the SU(3) flavor breaking c_1^V and c_2^V terms, $B_1 = B_2 = B_3 = B_4 = c_0^V$, and then all hadronic helicity amplitudes of $D \to V\ell^+\nu_\ell$ are related by only one parameter c_0^V or $A_1(0)$.

Among the $D \to V\ell^+\nu_\ell$ decay modes, 13 branching ratios have been measured, and 2 branching ratios have been upper limited by the experiments. The experimental data with 2σ errors are listed in the second column of Table 5. Now we use the listed experimental data to constrain the parameters B_i and then predict other not yet measured and not yet well measured branching ratios. The constrained form factor $A_1(0)$ is 0.638 ± 0.025, 0.605 ± 0.050 and 0.615 ± 0.020 in the C_1, C_2 and C_3 cases, respectively. The numerical results of $\mathcal{B}(D \to V\ell^+\nu_\ell)$ in the C_1, C_2, C_3 and C_4 cases are given in the third, fourth, fifth and sixth columns of Table 5, respectively.

The results in the C_1, C_2 and C_3 cases are very similar. Since the SU(3) flavor symmetry predictions of $\mathcal{B}(D^+ \to \omega e^+\nu_e)$ and $\mathcal{B}(D^0 \to \rho^-\mu^+\nu_\mu)$ are slightly larger than their experimental

Table 3
Quantities $\langle X\rangle$ and $\overline{X}$ of the $D \to P\ell^+\nu$ in the C_3 case. Note that some errors are tiny, so we only list the central values, the same below.

Decay modes	$\langle A_{FB}^{\ell}\rangle$	$\frac{\overline{A_{FB}^{e}}(\times 10^{-6})}{\overline{A_{FB}^{\mu,\tau}}(\times 10^{-2})}$	$\langle C_F^{\ell}\rangle$	$\overline{C_F^{\ell}}$	$\langle P_L^{\ell}\rangle$	$\overline{P_L^{\ell}}$	$\langle P_T^{\ell}\rangle$	$\frac{\overline{P_T^{e}}(\times 10^{-3})}{\overline{P_T^{\mu,\tau}}}$
$D^+ \to \overline{K}^0 e^+\nu_e$	-0.087	-3.254 ± 0.001	-1.239	-1.500	0.768	1.000	-0.273	-2.442 ± 0.001
$D^+ \to \pi^0 e^+\nu_e$	-0.083	-2.054 ± 0.000	-1.252	-1.500	0.780	1.000	-0.260	-1.730 ± 0.000
$D^+ \to \eta e^+\nu_e$	-0.087	-3.476 ± 0.001	-1.239	-1.500	0.768	1.000	-0.273	-2.490 ± 0.000
$D^+ \to \eta' e^+\nu_e$	-0.093	-7.075 ± 0.003	-1.222	-1.500	0.753	1.000	-0.290	-3.890 ± 0.001
$D^0 \to K^- e^+\nu_e$	-0.087	-3.259 ± 0.001	-1.239	-1.500	0.768	1.000	-0.273	-2.446 ± 0.001
$D^0 \to \pi^- e^+\nu_e$	-0.083	-2.077 ± 0.000	-1.252	-1.500	0.779	1.000	-0.260	-1.751 ± 0.000
$D_s^+ \to \eta e^+\nu_e$	-0.086	-3.033 ± 0.001	-1.242	-1.500	0.770	1.000	-0.270	-2.300 ± 0.001
$D_s^+ \to \eta' e^+\nu_e$	-0.091	-5.829 ± 0.003	-1.226	-1.500	0.757	1.000	-0.286	-3.484 ± 0.001
$D_s^+ \to K^0 e^+\nu_e$	-0.085	-2.814 ± 0.001	-1.245	-1.500	0.773	1.000	-0.267	-2.118 ± 0.000
$D_s^+ \to \pi^0 e^+\nu_e$	-0.082	-1.850 ± 0.001	-1.254	-1.500	0.781	1.000	-0.258	-1.634 ± 0.001
$D^+ \to \overline{K}^0 \mu^+\nu_\mu$	-0.226	-4.278 ± 0.001	-0.822	-1.352	0.394	0.851	-0.655	-0.414
$D^+ \to \pi^0 \mu^+\nu_\mu$	-0.201	-2.810 ± 0.000	-0.897	-1.405	0.462	0.907	-0.602	-0.310
$D^+ \to \eta \mu^+\nu_\mu$	-0.227	-4.490 ± 0.001	-0.819	-1.347	0.391	0.846	-0.657	-0.419
$D^+ \to \eta' \mu^+\nu_\mu$	-0.263	-8.097 ± 0.003	-0.708	-1.213	0.287	0.703	-0.725	-0.581
$D^0 \to K^- \mu^+\nu_\mu$	-0.226	-4.285 ± 0.001	-0.822	-1.352	0.393	0.850	-0.656	-0.414
$D^0 \to \pi^- \mu^+\nu_\mu$	-0.201	-2.844 ± 0.001	-0.895	-1.407	0.461	0.910	-0.603	-0.313
$D_s^+ \to \eta \mu^+\nu_\mu$	-0.221	-4.001 ± 0.001	-0.836	-1.364	0.406	0.864	-0.646	-0.394
$D_s^+ \to \eta' \mu^+\nu_\mu$	-0.254	-6.952 ± 0.003	-0.736	-1.254	0.314	0.747	-0.709	-0.540
$D_s^+ \to K^0 \mu^+\nu_\mu$	-0.215	-3.701 ± 0.001	-0.856	-1.377	0.425	0.879	-0.632	-0.367
$D_s^+ \to \pi^0 \mu^+\nu_\mu$	-0.197	-2.571 ± 0.001	-0.907	-1.417	0.472	0.920	-0.594	-0.295
$D_s^+ \to \pi^0 \tau^+\nu_\tau$	-0.281	-27.429 ± 0.105	-0.211 ± 0.003	-0.212 ± 0.003	-0.868 ± 0.001	-0.873 ± 0.001	-0.447 ± 0.002	-0.437 ± 0.002

Table 4
The hadronic helicity amplitudes for $D \to V\ell^+\nu$ decays including both the SU(3) flavor symmetry and the SU(3) flavor breaking contributions. $B_1 = c_0^V + c_1^V - 2c_2^V$, $B_2 = c_0^V - 2c_1^V - 2c_2^V$, $B_3 = c_0^V + c_1^V + c_2^V$, $B_4 = c_0^V - 2c_1^V + c_2^V$. If neglecting the SU(3) flavor breaking c_1^V and c_2^V terms, $B_1 = B_2 = B_3 = B_4 = c_0^V$.

Hadronic helicity amplitudes	SU(3) IRA amplitudes
$H(D^0 \to K^{*-}\ell^+\nu_\ell)$	$B_1 V_{cs}^*$
$H(D^+ \to \overline{K}^{*0}\ell^+\nu_\ell)$	$B_1 V_{cs}^*$
$H(D_s^+ \to \phi\ell^+\nu_\ell)$	$\left(-cos\theta_V\sqrt{2/3} - sin\theta_V/\sqrt{3}\right)B_2 V_{cs}^*$
$H(D_s^+ \to \omega\ell^+\nu_\ell)$	$\left(-sin\theta_V\sqrt{2/3} + cos\theta_V/\sqrt{3}\right)B_2 V_{cs}^*$
$H(D^0 \to \rho^-\ell^+\nu_\ell)$	$B_3 V_{cd}^*$
$H(D^+ \to \rho^0\ell^+\nu_\ell)$	$-\frac{1}{\sqrt{2}}B_3 V_{cd}^*$
$H(D^+ \to \phi\ell^+\nu_\ell)$	$\left(cos\theta_V/\sqrt{6} - sin\theta_V/\sqrt{3}\right)B_3 V_{cd}^*$
$H(D^+ \to \omega\ell^+\nu_\ell)$	$\left(sin\theta_V/\sqrt{6} + cos\theta_V/\sqrt{3}\right)B_3 V_{cd}^*$
$H(D_s^+ \to K^{*0}\ell^+\nu_\ell)$	$B_4 V_{cd}^*$

data within 2σ errors in the three cases, we do not use them to constrain the nonperturbative parameter c_0^V. One can see that the prediction of $\mathcal{B}(D^0 \to \rho^-\mu^+\nu_\mu)$ agree with its experimental data within 3σ errors, nevertheless, the prediction of $\mathcal{B}(D^+ \to \omega e^+\nu_e)$ still slightly larger than experimental data within 3σ errors. $\mathcal{B}(D_s^+ \to K^{*0}\mu^+\nu_\mu)$ and $\mathcal{B}(D_s^+ \to \omega e^+\nu_e, \omega\mu^+\nu_\mu)$ are predicted on the order of $\mathcal{O}(10^{-3})$ and $\mathcal{O}(10^{-5})$, respectively. And they could be measured in BESIII, LHCb and BelleII experiments. In the C_4 case, as given in the sixth column of Table 5, after considering both the hadronic momentum-transfer q^2 dependence of the form factors and the SU(3) flavor breaking contributions, all SU(3) flavor symmetry predictions are consis-

Table 5
Branching ratios of the $D \to V\ell^+\nu$ within 2σ errors. †The experimental data of $\mathcal{B}(D^+ \to \omega e^+\nu_e)$ and $\mathcal{B}(D^0 \to \rho^-\mu^+\nu_\mu)$ from PDG [1] are not used in the $C_{1,2,3}$ cases.

Branching ratios	Exp. data	Ones in C_1	Ones in C_2	Ones in C_3	Ones in C_4
$\mathcal{B}(D^+ \to \overline{K}^{*0}e^+\nu_e)(\times 10^{-2})$	5.40 ± 0.20	5.44 ± 0.15	5.42 ± 0.18	5.36 ± 0.08	5.44 ± 0.16
$\mathcal{B}(D^+ \to \rho^0 e^+\nu_e)(\times 10^{-3})$	$2.18^{+0.34}_{-0.50}$	2.31 ± 0.07	2.39 ± 0.13	2.33 ± 0.05	1.83 ± 0.15
$\mathcal{B}(D^+ \to \omega e^+\nu_e)(\times 10^{-3})$	1.69 ± 0.22	$2.24 \pm 0.07^\dagger$	$2.33 \pm 0.12^\dagger$	$2.26 \pm 0.04^\dagger$	1.77 ± 0.14
$\mathcal{B}(D^+ \to \phi e^+\nu_e)(\times 10^{-7})$	< 130	3.13 ± 0.12	3.11 ± 0.19	3.07 ± 0.07	2.38 ± 0.23
$\mathcal{B}(D^0 \to K^{*-}e^+\nu_e)(\times 10^{-2})$	2.15 ± 0.32	2.12 ± 0.09	2.13 ± 0.10	2.08 ± 0.06	2.13 ± 0.10
$\mathcal{B}(D^0 \to \rho^- e^+\nu_e)(\times 10^{-3})$	1.50 ± 0.24	1.79 ± 0.08	1.86 ± 0.11	1.80 ± 0.06	1.41 ± 0.13
$\mathcal{B}(D_s^+ \to \phi e^+\nu_e)(\times 10^{-2})$	2.39 ± 0.32	2.46 ± 0.12	2.43 ± 0.14	2.40 ± 0.10	2.39 ± 0.32
$\mathcal{B}(D_s^+ \to \omega e^+\nu_e)(\times 10^{-5})$	< 200	2.45 ± 0.13	2.56 ± 0.20	2.47 ± 0.10	2.49 ± 0.38
$\mathcal{B}(D_s^+ \to K^{*0}e^+\nu_e)(\times 10^{-3})$	2.15 ± 0.56	2.17 ± 0.10	2.25 ± 0.13	2.17 ± 0.08	2.15 ± 0.56
$\mathcal{B}(D^+ \to \overline{K}^{*0}\mu^+\nu_\mu)(\times 10^{-2})$	5.27 ± 0.30	5.12 ± 0.15	5.13 ± 0.16	5.05 ± 0.08	5.12 ± 0.15
$\mathcal{B}(D^+ \to \rho^0\mu^+\nu_\mu)(\times 10^{-3})$	2.4 ± 0.8	2.19 ± 0.07	2.29 ± 0.13	2.22 ± 0.04	1.74 ± 0.14
$\mathcal{B}(D^+ \to \omega\mu^+\nu_\mu)(\times 10^{-3})$	1.77 ± 0.42	2.13 ± 0.06	2.23 ± 0.12	2.15 ± 0.04	1.68 ± 0.13
$\mathcal{B}(D^+ \to \phi\mu^+\nu_\mu)(\times 10^{-7})$	$\cdots$	2.89 ± 0.11	2.89 ± 0.17	2.84 ± 0.07	2.20 ± 0.21
$\mathcal{B}(D^0 \to K^{*-}\mu^+\nu_\mu)(\times 10^{-2})$	1.89 ± 0.48	1.99 ± 0.09	2.01 ± 0.09	1.96 ± 0.06	2.01 ± 0.10
$\mathcal{B}(D^0 \to \rho^-\mu^+\nu_\mu)(\times 10^{-3})$	1.35 ± 0.26	$1.70 \pm 0.07^\dagger$	$1.78 \pm 0.11^\dagger$	$1.72 \pm 0.06^\dagger$	1.34 ± 0.13
$\mathcal{B}(D_s^+ \to \phi\mu^+\nu_\mu)(\times 10^{-2})$	1.9 ± 1.0	2.30 ± 0.12	2.29 ± 0.12	2.25 ± 0.09	2.24 ± 0.30
$\mathcal{B}(D_s^+ \to \omega\mu^+\nu_\mu)(\times 10^{-5})$	$\cdots$	2.34 ± 0.12	2.47 ± 0.19	2.37 ± 0.09	2.38 ± 0.36
$\mathcal{B}(D_s^+ \to K^{*0}\mu^+\nu_\mu)(\times 10^{-3})$	$\cdots$	2.06 ± 0.10	2.15 ± 0.13	2.07 ± 0.08	2.05 ± 0.53

tent with their experimental data within 2σ errors. Among relevant not yet measured decays, $\mathcal{B}(D_s^+ \to K^{*0}\mu^+\nu_\mu)$ is calculated in the SM using light-cone sum rules [88] and in the relativistic quark model [7], $\mathcal{B}(D_s^+ \to K^{*0}\mu^+\nu_\mu) = (2.23 \pm 0.32) \times 10^{-3}$ [88] and 2.0×10^{-3} [7], and our predictions of $\mathcal{B}(D_s^+ \to K^{*0}\mu^+\nu_\mu)$ in the C_1, C_2, C_3 and C_4 cases are coincident with previous ones in Refs. [7,88]. In addition, the lepton flavor universality parameters $R^{\mu/e}(D \to V\ell^+\nu_\ell) \equiv \frac{\mathcal{B}(D\to V\mu^+\nu_\mu)}{\mathcal{B}(D\to Ve^+\nu_e)}$ have also been studied in this work. Since many terms are canceled in the ratios, these predictions of the lepton flavor universality parameters are quite accurate, our predictions in all four cases are similar to each other, and all $R^{\mu/e}(D \to V\ell^+\nu_\ell)$ lie in $[0.92, 0.97]$.

For the q^2 dependence of the differential branching ratios of the $D \to V\ell^+\nu_\ell$ decays with present experimental bounds, we only show the not yet measured processes $D^+ \to \phi\mu^+\nu_\mu$, $D_s^+ \to \omega\mu^+\nu_\mu$ and $D_s^+ \to K^{*0}\mu^+\nu_\mu$ in Fig. 3. The differential branching ratios of $D^+ \to \phi e^+\nu_e$ ($D_s^+ \to \omega e^+\nu_e$) are similar to $D^+ \to \phi\mu^+\nu_\mu$ ($D_s^+ \to \omega\mu^+\nu_\mu$), so we do not shown them in Fig. 3. From Fig. 3, one can see that present experimental data give quite strong bounds on all differential branching ratios of $D^+ \to \phi\mu^+\nu_\mu$, $D_s^+ \to \omega\mu^+\nu_\mu$ and $D_s^+ \to K^{*0}\mu^+\nu_\mu$ decays in the C_1, C_2 and C_3 cases. The prediction of $d\mathcal{B}(D^+ \to \phi\mu^+\nu_\mu)/dq^2$ in the C_4 case could be distinguished from ones in the $C_{1,2,3}$ cases within the middle range of q^2. And the error of $d\mathcal{B}(D_s^+ \to K^{*0}\mu^+\nu_\mu)/dq^2$ in the C_4 case is obviously larger than ones in the $C_{1,2,3}$ cases.

The forward-backward asymmetries A_{FB}^ℓ, the lepton-side convexity parameters C_F^ℓ, the longitudinal polarizations P_L^ℓ, the transverse polarizations P_T^ℓ, the lepton spin asymmetries A_λ and the longitudinal polarization fractions of the final vector mesons F_L with two ways of integration have also been predicted in the four cases. Since many theoretical uncertainties are canceled in the ratios, these predictions are very accurate. These predictions are similar to each other in the four cases, and we only list the results in the C_3 case in Tables 6-7 for examples. One can see

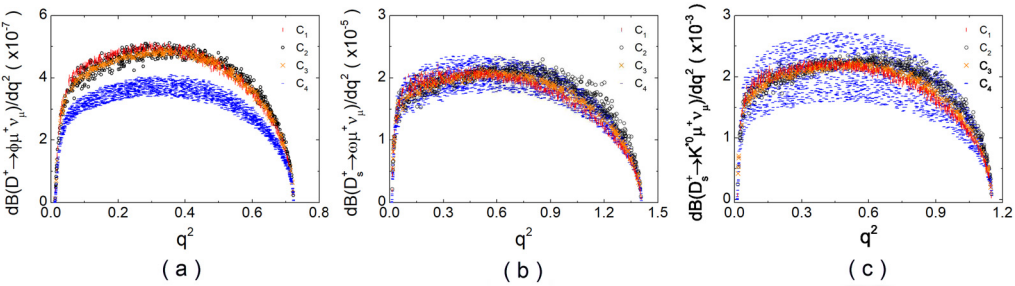

Fig. 3. The q^2 dependence of the differential branching ratios for some not yet measured $D \to V\mu^+\nu_\mu$ decays with present experimental bounds.

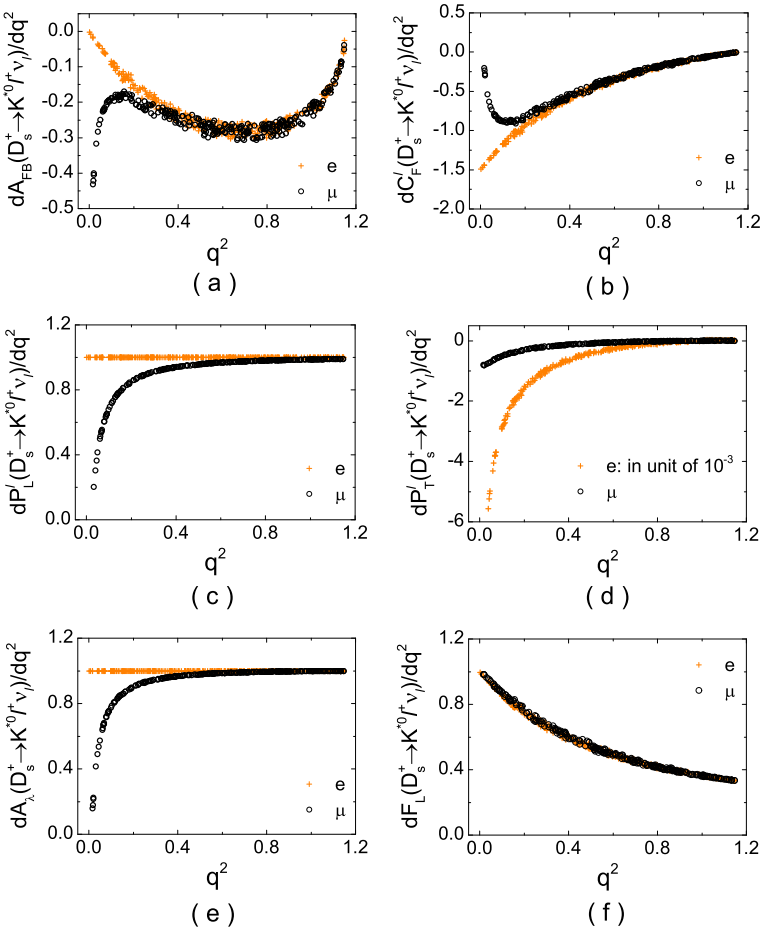

Fig. 4. The differential forward-backward asymmetries, differential lepton-side convexity parameters, differential longitudinal lepton polarizations and differential transverse lepton polarizations for the $D_s^+ \to K^{*0}\ell^+\nu_\ell$ decays in the C_3 case.

Table 6
The forward-backward asymmetries A_{FB}^{ℓ}, the lepton-side convexity parameters C_F^{ℓ}, the longitudinal polarizations P_L^{ℓ} of the $D \to V\ell^+\nu$ decays in the C_3 case.

Decay modes	$\langle A_{FB}^{\ell}\rangle$	$\overline{A_{FB}^{\ell}}$	$\langle C_F^{\ell}\rangle$	$\overline{C_F^{\ell}}$	$\langle P_L^{\ell}\rangle$	$\overline{P_L^{\ell}}$
$D^+ \to \overline{K}^{*0} e^+ \nu_e$	-0.125 ± 0.006	-0.190 ± 0.020	-1.046 ± 0.019	-0.500 ± 0.032	0.786 ± 0.004	1.000
$D^+ \to \rho^0 e^+ \nu_e$	-0.130 ± 0.008	-0.222 ± 0.024	-1.052 ± 0.023	-0.496 ± 0.041	0.789 ± 0.004	1.000
$D^+ \to \omega e^+ \nu_e$	-0.130 ± 0.008	-0.220 ± 0.024	-1.052 ± 0.023	-0.497 ± 0.041	0.789 ± 0.004	1.000
$D^+ \to \phi e^+ \nu_e$	-0.121 ± 0.005	-0.164 ± 0.017	-1.037 ± 0.015	-0.500 ± 0.025	0.784 ± 0.003	1.000
$D^0 \to K^{*-} e^+ \nu_e$	-0.125 ± 0.006	-0.191 ± 0.020	-1.046 ± 0.019	-0.500 ± 0.032	0.786 ± 0.004	1.000
$D^0 \to \rho^- e^+ \nu_e$	-0.130 ± 0.008	-0.221 ± 0.024	-1.052 ± 0.023	-0.497 ± 0.041	0.789 ± 0.004	1.000
$D_s^+ \to \phi e^+ \nu_e$	-0.122 ± 0.006	-0.176 ± 0.018	-1.043 ± 0.016	-0.500 ± 0.028	0.786 ± 0.003	1.000
$D_s^+ \to \omega e^+ \nu_e$	-0.130 ± 0.008	-0.229 ± 0.025	-1.057 ± 0.025	-0.496 ± 0.044	0.790 ± 0.004	1.000
$D_s^+ \to K^{*0} e^+ \nu_e$	-0.128 ± 0.007	-0.207 ± 0.022	-1.049 ± 0.021	-0.495 ± 0.036	0.789 ± 0.004	1.000
$D^+ \to \overline{K}^{*0} \mu^+ \nu_\mu$	-0.284 ± 0.009	-0.226 ± 0.019	-0.466 ± 0.021	-0.395 ± 0.028	0.514 ± 0.017	0.886 ± 0.002
$D^+ \to \rho^0 \mu^+ \nu_\mu$	-0.292 ± 0.011	-0.252 ± 0.023	-0.491 ± 0.027	-0.405 ± 0.037	0.524 ± 0.020	0.903 ± 0.002
$D^+ \to \omega \mu^+ \nu_\mu$	-0.292 ± 0.011	-0.251 ± 0.022	-0.490 ± 0.027	-0.405 ± 0.037	0.524 ± 0.020	0.902 ± 0.002
$D^+ \to \phi \mu^+ \nu_\mu$	-0.277 ± 0.008	-0.206 ± 0.016	-0.433 ± 0.016	-0.376 ± 0.021	0.503 ± 0.014	0.864 ± 0.002
$D^0 \to K^{*-} \mu^+ \nu_\mu$	-0.284 ± 0.009	-0.226 ± 0.019	-0.466 ± 0.021	-0.395 ± 0.029	0.514 ± 0.017	0.886 ± 0.002
$D^0 \to \rho^- \mu^+ \nu_\mu$	-0.292 ± 0.011	-0.252 ± 0.023	-0.490 ± 0.027	-0.405 ± 0.037	0.524 ± 0.020	0.902 ± 0.002
$D_s^+ \to \phi \mu^+ \nu_\mu$	-0.277 ± 0.008	-0.213 ± 0.017	-0.459 ± 0.018	-0.391 ± 0.024	0.514 ± 0.015	0.882 ± 0.002
$D_s^+ \to \omega \mu^+ \nu_\mu$	-0.291 ± 0.012	-0.257 ± 0.024	-0.509 ± 0.029	-0.414 ± 0.041	0.531 ± 0.021	0.913 ± 0.002
$D_s^+ \to K^{*0} \mu^+ \nu_\mu$	-0.286 ± 0.010	-0.239 ± 0.021	-0.485 ± 0.024	-0.402 ± 0.033	0.525 ± 0.018	0.900 ± 0.002

Table 7
The transverse polarizations P_T^{ℓ}, the lepton spin asymmetries A_λ and the longitudinal polarization fractions of the final vector mesons F_L of the $D \to V\ell^+\nu$ decays in the C_3 case.

Decay modes	$\langle P_T^{\ell}\rangle$	$\frac{\overline{P_T^e}(\times 10^{-3})}{\overline{P_T^\mu}}$	$\langle A_\lambda\rangle$	$\overline{A_\lambda}$	$\langle F_L\rangle$	$\overline{F_L}$
$D^+ \to \overline{K}^{*0} e^+ \nu_e$	-0.251 ± 0.004	-1.205 ± 0.066	1.000	1.000	0.905 ± 0.010	0.556 ± 0.014
$D^+ \to \rho^0 e^+ \nu_e$	-0.249 ± 0.005	-1.040 ± 0.072	1.000	1.000	0.907 ± 0.012	0.554 ± 0.018
$D^+ \to \omega e^+ \nu_e$	-0.249 ± 0.005	-1.049 ± 0.073	1.000	1.000	0.907 ± 0.012	0.554 ± 0.018
$D^+ \to \phi e^+ \nu_e$	-0.254 ± 0.003	-1.417 ± 0.061	1.000	1.000	0.902 ± 0.008	0.556 ± 0.011
$D^0 \to K^{*-} e^+ \nu_e$	-0.251 ± 0.004	-1.206 ± 0.067	1.000	1.000	0.905 ± 0.010	0.556 ± 0.014
$D^0 \to \rho^- e^+ \nu_e$	-0.249 ± 0.005	-1.045 ± 0.073	1.000	1.000	0.907 ± 0.012	0.554 ± 0.018
$D_s^+ \to \phi e^+ \nu_e$	-0.251 ± 0.004	-1.255 ± 0.060	1.000	1.000	0.904 ± 0.009	0.555 ± 0.012
$D_s^+ \to \omega e^+ \nu_e$	-0.247 ± 0.005	-0.953 ± 0.071	1.000	1.000	0.908 ± 0.013	0.554 ± 0.020
$D_s^+ \to K^{*0} e^+ \nu_e$	-0.248 ± 0.004	-1.075 ± 0.066	1.000	1.000	0.905 ± 0.011	0.553 ± 0.016
$D^+ \to \overline{K}^{*0} \mu^+ \nu_\mu$	-0.454 ± 0.022	-0.156 ± 0.012	0.935 ± 0.005	0.928 ± 0.002	0.775 ± 0.019	0.557 ± 0.014
$D^+ \to \rho^0 \mu^+ \nu_\mu$	-0.452 ± 0.026	-0.139 ± 0.014	0.944 ± 0.006	0.937 ± 0.002	0.782 ± 0.023	0.555 ± 0.018
$D^+ \to \omega \mu^+ \nu_\mu$	-0.452 ± 0.026	-0.140 ± 0.014	0.944 ± 0.006	0.937 ± 0.002	0.782 ± 0.023	0.555 ± 0.018
$D^+ \to \phi \mu^+ \nu_\mu$	-0.455 ± 0.018	-0.175 ± 0.011	0.924 ± 0.005	0.915 ± 0.002	0.763 ± 0.015	0.557 ± 0.011
$D^0 \to K^{*-} \mu^+ \nu_\mu$	-0.454 ± 0.022	-0.156 ± 0.012	0.935 ± 0.005	0.927 ± 0.002	0.775 ± 0.019	0.557 ± 0.014
$D^0 \to \rho^- \mu^+ \nu_\mu$	-0.452 ± 0.026	-0.140 ± 0.014	0.944 ± 0.006	0.937 ± 0.002	0.782 ± 0.023	0.555 ± 0.018
$D_s^+ \to \phi \mu^+ \nu_\mu$	-0.454 ± 0.019	-0.162 ± 0.011	0.934 ± 0.005	0.925 ± 0.002	0.771 ± 0.016	0.557 ± 0.012
$D_s^+ \to \omega \mu^+ \nu_\mu$	-0.452 ± 0.027	-0.131 ± 0.014	0.950 ± 0.005	0.943 ± 0.002	0.788 ± 0.024	0.555 ± 0.019
$D_s^+ \to K^{*0} \mu^+ \nu_\mu$	-0.451 ± 0.023	-0.143 ± 0.012	0.943 ± 0.005	0.936 ± 0.002	0.779 ± 0.021	0.555 ± 0.016

that the predictions are obviously different between two ways of q^2 integration, and they are also quite different between $D \to Ve^+\nu_e$ and $D \to V\mu^+\nu_\mu$ decays.

The differential observables of $D_s^+ \to K^{*0}\ell^+\nu_\ell$ decays in the C_3 case are displayed in Fig. 4. One can see that, in the low q^2 ranges, the differential observables expect $dF_L(D_s^+ \to K^{*0}\ell^+\nu_\ell)/dq^2$ are obviously different between decays with $\ell = e$ and $\ell = \mu$.

Table 8
The hadronic helicity amplitudes for the $D \to S\ell^+\nu$ decays including both the SU(3) flavor symmetry and the SU(3) flavor breaking contributions. In the two quark picture of the scalar mesons, $E_1 \equiv c_0^S + c_1^S - 2c_2^S$, $E_2 \equiv c_0^S - 2c_1^S - 2c_2^S$, $E_3 \equiv c_0^S + c_1^S + c_2^S$, $E_4 \equiv c_0^S - 2c_1^S + c_2^S$, and $E_1 = E_2 = E_3 = E_4 = c_0^S$ if neglecting the SU(3) flavor breaking c_1^S and c_2^S terms. In the four quark picture of the scalar mesons, $E'_1 \equiv c_0'^S + c_1'^S - 2c_2'^S + c_3'^S$, $E'_2 \equiv c_0'^S - 2c_1'^S - 2c_2'^S + c_3'^S$, $E'_3 \equiv c_0'^S + c_1'^S + c_2'^S - 2c_3'^S$, $E'_4 \equiv c_0'^S + c_1'^S + c_2'^S + c_3'^S$, $E'_5 \equiv c_0'^S - 2c_1'^S + c_2'^S + c_3'^S$, and $E'_1 = E'_2 = E'_3 = E'_4 = E'_5 = c_0'^S$ if neglecting the SU(3) flavor breaking $c_1'^S$, $c_2'^S$ and $c_3'^S$ terms.

Hadronic helicity amplitudes	ones for two-quark scenario	ones for four-quark scenario
$H(D^0 \to K_0^-\ell^+\nu_\ell)$	$E_1 V_{cs}^*$	$E'_1 V_{cs}^*$
$H(D^+ \to \overline{K}_0^0\ell^+\nu_\ell)$	$E_1 V_{cs}^*$	$E'_1 V_{cs}^*$
$H(D_s^+ \to f_0\ell^+\nu_\ell)$	$E_2 V_{cs}^*$	$\sqrt{2}E'_2 V_{cs}^*$
$H(D_s^+ \to f_0(980)\ell^+\nu_\ell)$	$cos\theta_S\ E_2 V_{cs}^*$	$\sqrt{2}cos\phi_S\ E'_2 V_{cs}^*$
$H(D_s^+ \to f_0(500)\ell^+\nu_\ell)$	$-sin\theta_S\ E_2 V_{cs}^*$	$-\sqrt{2}sin\phi_S\ E'_2 V_{cs}^*$
$H(D^0 \to a_0^-\ell^+\nu_\ell)$	$E_3 V_{cd}^*$	$E'_3 V_{cd}^*$
$H(D^+ \to a_0^0\ell^+\nu_\ell)$	$-\frac{1}{\sqrt{2}}E_3 V_{cd}^*$	$-\frac{1}{\sqrt{2}}E'_3 V_{cd}^*$
$H(D^+ \to f_0\ell^+\nu_\ell)$	0	$\frac{1}{\sqrt{2}}E'_3 V_{cd}^*$
$H(D^+ \to \sigma\ell^+\nu_\ell)$	$\frac{1}{\sqrt{2}}E_3 V_{cd}^*$	$E'_4 V_{cd}^*$
$H(D^+ \to f_0(980)\ell^+\nu_\ell)$	$\frac{1}{\sqrt{2}}sin\theta_S\ E_3 V_{cd}^*$	$(\frac{1}{\sqrt{2}}E'_3 cos\phi_S + E'_4 sin\phi_S)V_{cd}^*$
$H(D^+ \to f_0(500)\ell^+\nu_\ell)$	$\frac{1}{\sqrt{2}}cos\theta_S\ E_3 V_{cd}^*$	$(-\frac{1}{\sqrt{2}}E'_3 sin\phi_S + E'_4 cos\phi_S)V_{cd}^*$
$H(D_s^+ \to K_0^0\ell^+\nu_\ell)$	$E_4 V_{cd}^*$	$E'_5 V_{cd}^*$

3.3. $D \to S\ell^+\nu_\ell$ decays

For $D \to S\ell^+\nu_\ell$ decays, the two quark and the four quark scenarios for the scalar mesons below or near 1 GeV are considered. The hadronic helicity amplitudes for the $D \to S\ell^+\nu_\ell$ decays are given in Table 8, in which the CKM matrix element V_{cs} and V_{cd} information are kept for comparing conveniently. There are four (five) nonperturbative parameters $E_{1,2,3,4}$ ($E'_{1,2,3,4,5}$) in the two quark (four quark) picture. After ignoring the SU(3) flavor breaking contributions, only one nonperturbative parameter $E_1 = E_2 = E_3 = E_4 = c_0^S$ or $E'_1 = E'_2 = E'_3 = E'_4 = E'_5 = c_0'^S$ relates all decay amplitudes in the two quark or the four quark picture, respectively.

Unlike many measured decay modes in the $D \to P\ell^+\nu_\ell$ and $D \to V\ell^+\nu_\ell$ decays, among these $D \to S\ell^+\nu_\ell$ decays, only $D_s^+ \to f_0(980)e^+\nu_e$ decay has been measured, and its branching ratio with 2σ errors is [1]

$$\mathcal{B}(D_s^+ \to f_0(980)e^+\nu_e) = (2.3 \pm 0.8) \times 10^{-3}. \tag{48}$$

In addition, the branching ratios of the $D \to P_1P_2\ell^+\nu_\ell$ decays with the light scalar resonances can be obtained by using $\mathcal{B}(D \to S\ell^+\nu_\ell)$ and $\mathcal{B}(S \to P_1P_2)$, and the detail analysis can be found in Ref. [89]. Five branching ratios and two upper limits of $\mathcal{B}(D \to S\ell^+\nu_\ell,\ S \to P_1P_2)$ have been measured, and the data within 2σ errors are ([1,90–92])

$$\mathcal{B}(D_s^+ \to f_0(980)e^+\nu_e,\ f_0(980) \to \pi^+\pi^-) = (1.30 \pm 0.63) \times 10^{-3}\ \ [90],$$
$$\mathcal{B}(D_s^+ \to f_0(980)e^+\nu_e,\ f_0(980) \to \pi^0\pi^0) = (7.9 \pm 2.9) \times 10^{-4}\ \ [91],$$
$$\mathcal{B}(D^0 \to a_0(980)^-e^+\nu_e,\ a_0(980)^- \to \eta\pi^-) = (1.33^{+0.68}_{-0.60}) \times 10^{-4}\ \ [1],$$
$$\mathcal{B}(D^+ \to a_0(980)^0e^+\nu_e,\ a_0(980)^0 \to \eta\pi^0) = (1.7^{+1.6}_{-1.4}) \times 10^{-4}\ \ [1],$$

$$\mathcal{B}(D^+ \to f_0(500)e^+\nu_e,\ f_0(500) \to \pi^+\pi^-) = (6.3 \pm 1.0) \times 10^{-4}\ \ [1],$$
$$\mathcal{B}(D^+ \to f_0(980)e^+\nu_e,\ f_0(980) \to \pi^+\pi^-) < 2.8 \times 10^{-5}\ \ [92],$$
$$\mathcal{B}(D_s^+ \to f_0(500)e^+\nu_e,\ f_0(500) \to \pi^0\pi^0) < 6.4 \times 10^{-4}\ \ [91]. \tag{49}$$

Two cases S_1 and S_2 will be considered in the $D \to S\ell^+\nu_\ell$ decays. In the S_1 case, only experimental datum of $\mathcal{B}(D_s^+ \to f_0(980)e^+\nu_e)$ is used to constrain one parameter $f_+^S(0)$ (*i.e.*, c_0^S or $c_0'^S$) and then predict other not yet measured branching ratios. The numerical results of $\mathcal{B}(D \to S\ell^+\nu)$ in the S_1 case are given in the 2-4th and 8th columns of Table 9. In the S_2 case, the experimental data of both $\mathcal{B}(D_s^+ \to f_0(980)e^+\nu_e)$ in Eq. (48) and $\mathcal{B}(D \to S\ell^+\nu_\ell,\ S \to P_1P_2)$ in Eq. (49) will be used to constrain the parameter c_0^S or $c_0'^S$. The predictions of $\mathcal{B}(D \to S\ell^+\nu)$ in the S_2 case are listed in the 5-7th and 9th columns of Table 9. Our comments on the results in the $S_{1,2}$ cases are as follows.

- **Results in the two quark picture:** In the two quark picture, the three possible ranges of the mixing angle, $25^\circ < \theta_S < 40^\circ$, $140^\circ < \theta_S < 165^\circ$ and $-30^\circ < \theta_S < 30^\circ$ [61,71] have been analyzed. In S_1 case, using the data of $\mathcal{B}(D_s^+ \to f_0(980)e^+\nu_e)$, we obtain the constrained form factor $f_+^S(0)$ is 0.098 ± 0.031, 0.094 ± 0.033 and 0.087 ± 0.027 with $25^\circ < \theta_S < 40^\circ$, $140^\circ < \theta_S < 165^\circ$ and $-30^\circ < \theta_S < 30^\circ$, respectively. And then many predictions of $\mathcal{B}(D \to S\ell^+\nu)$ are obtained. As given in the 2-4th columns of Table 9, one can see that the predictions with $25^\circ < \theta_S < 40^\circ$ are similar to ones with $140^\circ < \theta_S < 165^\circ$, the predictions with $-30^\circ < \theta_S < 30^\circ$ are slightly different from the first two, and the errors of predictions are quite large. After adding the experimental bounds of $\mathcal{B}(D \to S\ell^+\nu_\ell,\ S \to P_1P_2)$, as given in the 5-7th columns of Table 9, the three possible ranges of the mixing angle θ_S are obviously constrained, and they reduce to $25^\circ < \theta_S < 35^\circ$, $144^\circ < \theta_S < 158^\circ$ and $22^\circ \leq |\theta_S| \leq 30^\circ$, respectively. The form factor $f_+^S(0)$ is further constrained to 0.096 ± 0.010, 0.096 ± 0.011 and 0.096 ± 0.011 with $25^\circ < \theta_S < 35^\circ$, $144^\circ < \theta_S < 158^\circ$ and $22^\circ \leq |\theta_S| \leq 30^\circ$, respectively. In addition, the error of every prediction becomes smaller by adding the experimental bounds of $\mathcal{B}(D \to S\ell^+\nu_\ell,\ S \to P_1P_2)$.
- **Results in the four quark picture:** In the four quark picture, the constrained $f_+^S(0)$ is 0.057 ± 0.015 in the case S_1, and the predictions are listed in the 8-9th columns of Table 9. The majority of predictions in four quark picture are smaller than corresponding ones in two quark picture. Strong coupling constants g_4' and g_4 are appeared in $S \to P_1P_2$ decays with the four quark picture of light scalar mesons. At present, we only can determine $\left|\frac{g_4'}{g_4}\right|$ from the $S \to P_1P_2$ decays. The results of involved decays with both $\frac{g_4'}{g_4} > 0$ and $\frac{g_4'}{g_4} < 0$ are given in the 9th column of Table 9, and one can see that, except $\mathcal{B}(D_s^+ \to f_0(500)e^+\nu_e)$ and $\mathcal{B}(D_s^+ \to f_0(980)\mu^+\nu_\mu)$, the other involved branching ratios are not obviously affected by the choice of $\frac{g_4'}{g_4} > 0$ or $\frac{g_4'}{g_4} < 0$. The constrained $f_+^S(0)$ shrinks to 0.063 ± 0.009 and the errors of the branching ratio predictions are obviously reduced by the experimental bounds of $\mathcal{B}(D \to S\ell^+\nu_\ell,\ S \to P_1P_2)$.
- **Comparing with previous predictions:** Previous predictions are listed in the last column of Table 9. $\mathcal{B}(D_s^+ \to f_0(500)e^+\nu_e)$, $\mathcal{B}(D_s^+ \to f_0(500)\mu^+\nu_\mu)$ and $\mathcal{B}(D^+ \to f_0(500)\mu^+\nu_\mu)$ are predicted for the first time. Our predictions of $\mathcal{B}(D_s^+ \to f_0(980)\mu^+\nu_\mu)$, $\mathcal{B}(D^+ \to a_0^0e^+\nu_e)$, $\mathcal{B}(D^+ \to f_0(980)e^+\nu_e)$, $\mathcal{B}(D^+ \to f_0(500)e^+\nu_e)$ and $\mathcal{B}(D^+ \to a_0^0\mu^+\nu_\mu)$ are consistent with previous predictions in Refs. [87,93,94]. Our other predictions are about one order smaller or one order larger than previous ones in Refs. [70,95].

Table 9
Branching ratios of $D \to S\ell^+\nu$ decays within 2σ errors. As given in Ref. [89], g_4' and g_4 are strong coupling constants obtained by the SU(3) flavor symmetry in $S \to P_1 P_2$ decays, ^{a}denotes the results with $\frac{g_4'}{g_4} > 0$, and ^{b}denotes ones with $\frac{g_4'}{g_4} < 0$, †denotes the results with two quark picture, and ‡denotes the results with four quark picture.

Branching ratios	ones for $2q$ state in S_1			ones for $2q$ state in S_2			ones for $4q$	ones for $4q$	Previous ones
	$[25°, 40°]$	$[140°, 165°]$	$[-30°, 30°]$	$[25°, 35°]$	$[144°, 158°]$	$22° \le \lvert\theta_S\rvert \le 30°$	state in S_1	state in S_2	
$\mathcal{B}(D^0 \to K_0^- e^+\nu_e)(\times 10^{-3})$	3.38 ± 2.12	3.18 ± 2.05	2.57 ± 1.58	3.02 ± 1.11	3.00 ± 1.10	2.98 ± 1.05	1.11 ± 0.63	1.25 ± 0.45	$0.103 \pm 0.115^\dagger$ [70]
$\mathcal{B}(D^+ \to \overline{K}_0^0 e^+\nu_e)(\times 10^{-3})$	8.66 ± 5.55	7.99 ± 5.02	7.02 ± 4.48	7.74 ± 2.88	7.78 ± 2.77	7.68 ± 2.78	2.85 ± 1.65	3.36 ± 1.25	$38.8 \pm 5.6^\dagger$ [70]
$\mathcal{B}(D_s^+ \to f_0(980) e^+\nu_e)(\times 10^{-3})$	2.30 ± 0.80	2.30 ± 0.80	2.30 ± 0.80	2.58 ± 0.52	2.57 ± 0.53	2.71 ± 0.39	2.30 ± 0.80	$^{2.49\pm0.61}_{2.54\pm0.56}{}^a$	$2.1 \pm 0.2^\dagger$ [87], $2^{+0.5\dagger}_{-0.4}$ [93]
$\mathcal{B}(D_s^+ \to f_0(500) e^+\nu_e)(\times 10^{-3})$	6.73 ± 6.11	5.98 ± 5.75	3.25 ± 3.25	1.49 ± 0.43	1.45 ± 0.46	1.42 ± 0.50	0.37 ± 0.37	$^{0.31\pm0.31}_{0.17\pm0.17}{}^b$	
$\mathcal{B}(D^0 \to K_0^- \mu^+\nu_\mu)(\times 10^{-3})$	2.90 ± 1.84	2.73 ± 1.77	2.20 ± 1.36	2.59 ± 0.97	2.57 ± 0.96	2.56 ± 0.92	0.95 ± 0.54	1.09 ± 0.39	$0.103 \pm 0.115^\dagger$ [70]
$\mathcal{B}(D^+ \to \overline{K}_0^0 \mu^+\nu_\mu)(\times 10^{-3})$	7.46 ± 4.81	6.87 ± 4.33	6.04 ± 3.88	6.65 ± 2.52	6.69 ± 2.43	6.59 ± 2.43	2.45 ± 1.43	2.89 ± 1.09	$38.8 \pm 5.6^\dagger$ [70]
$\mathcal{B}(D_s^+ \to f_0(980) \mu^+\nu_\mu)(\times 10^{-3})$	1.95 ± 0.70	1.95 ± 0.70	1.95 ± 0.69	2.20 ± 0.45	2.20 ± 0.45	2.32 ± 0.33	1.95 ± 0.70	$^{2.12\pm0.54}_{2.16\pm0.49}{}^a$	$2.1 \pm 0.2^\dagger$ [87]
$\mathcal{B}(D_s^+ \to f_0(500) \mu^+\nu_\mu)(\times 10^{-3})$	6.21 ± 5.66	5.53 ± 5.32	3.01 ± 3.01	1.33 ± 0.39	1.31 ± 0.43	1.28 ± 0.46	0.34 ± 0.34	$^{0.29\pm0.29}_{0.16\pm0.16}{}^b$	
$\mathcal{B}(D^0 \to a_0^- e^+\nu_e)(\times 10^{-5})$	9.99 ± 6.54	9.56 ± 6.50	8.34 ± 5.67	9.22 ± 3.98	9.09 ± 3.65	9.17 ± 3.58	3.42 ± 2.06	4.32 ± 1.17	$16.8 \pm 1.5^\dagger$ [87], $40.8^{+13.7\dagger}_{-12.2}$ [95], $24.4 \pm 3.0^\dagger$ [70]
$\mathcal{B}(D^+ \to a_0^0 e^+\nu_e)(\times 10^{-5})$	13.09 ± 8.62	12.62 ± 8.67	10.89 ± 7.35	12.09 ± 5.19	11.81 ± 4.71	11.97 ± 4.66	4.49 ± 2.71	5.68 ± 1.52	$21.8 \pm 3.8^\dagger$ [87], $54.0^{+17.8\ddagger}_{-15.9}$ [95] $6 \sim 8^\dagger$ [94], $5 \sim 5.4^\ddagger$ [94]
$\mathcal{B}(D^+ \to f_0(980) e^+\nu_e)(\times 10^{-5})$	3.92 ± 2.92	3.48 ± 3.13	1.59 ± 1.59	2.62 ± 0.82	2.52 ± 0.94	2.40 ± 0.80	3.14 ± 1.98	$^{3.35\pm1.80}_{3.89\pm1.35}{}^a$	$7.78 \pm 0.68^\dagger$ [87], $5.7 \pm 1.3^\dagger$ [96] $0.4 \sim 3.5^\dagger$ [94], $1.9 \sim 6.3^\ddagger$ [94]
$\mathcal{B}(D^+ \to f_0(500) e^+\nu_e)(\times 10^{-4})$	4.05 ± 3.20	4.08 ± 3.10	4.21 ± 3.28	2.16 ± 0.96	2.59 ± 1.38	2.70 ± 1.28	4.97 ± 4.13	$^{4.97\pm3.34}_{4.95\pm3.36}{}^a$	$0.4 \sim 0.6^\dagger$ [94], $0.88 \sim 1.4^\ddagger$ [94]
$\mathcal{B}(D^+ \to K_0^0 e^+\nu_e)(\times 10^{-4})$	3.73 ± 2.37	3.41 ± 2.13	2.99 ± 1.88	3.35 ± 1.21	3.32 ± 1.20	3.35 ± 1.15	1.25 ± 0.71	1.43 ± 0.51	$26.5 \pm 2.8^\dagger$ [70]
$\mathcal{B}(D^0 \to a_0^0 \mu^+\nu_\mu)(\times 10^{-5})$	8.25 ± 5.45	7.89 ± 5.42	6.91 ± 4.75	7.61 ± 3.37	7.51 ± 3.10	7.57 ± 3.04	2.83 ± 1.72	3.57 ± 0.99	$16.3 \pm 1.4^\dagger$ [87], $24.4 \pm 3.0^\dagger$ [70]
$\mathcal{B}(D^+ \to a_0^0 \mu^+\nu_\mu)(\times 10^{-5})$	10.83 ± 7.19	10.44 ± 7.23	9.04 ± 6.16	10.00 ± 4.41	9.76 ± 4.00	9.89 ± 3.97	3.73 ± 2.28	4.69 ± 1.30	$21.2 \pm 3.7^\dagger$ [87]
$\mathcal{B}(D^+ \to f_0(980) \mu^+\nu_\mu)(\times 10^{-5})$	3.23 ± 2.41	2.88 ± 2.60	1.32 ± 1.32	2.15 ± 0.70	2.09 ± 0.78	1.99 ± 0.66	2.56 ± 1.62	$^{2.74\pm1.49}_{3.20\pm1.14}{}^a$	$7.87 \pm 0.67^\dagger$ [87]
$\mathcal{B}(D^+ \to f_0(500) \mu^+\nu_\mu)(\times 10^{-4})$	3.69 ± 2.96	3.71 ± 2.86	3.84 ± 3.04	1.92 ± 0.88	2.32 ± 1.27	2.42 ± 1.19	4.54 ± 3.81	$^{4.52\pm3.10}_{4.49\pm3.12}{}^b$	
$\mathcal{B}(D_s^+ \to K_0^0 \mu^+\nu_\mu)(\times 10^{-4})$	3.28 ± 2.10	3.00 ± 1.88	2.62 ± 1.66	2.94 ± 1.08	2.91 ± 1.06	2.94 ± 1.02	1.10 ± 0.63	1.26 ± 0.45	$26.5 \pm 2.8^\dagger$ [70]

4. Summary

Many semileptonic $D \to P/V/S\ell^+\nu_\ell$ decays have been measured, and these processes could be used to test the SU(3) flavor symmetry approach. In terms of the SU(3) flavor symmetry and the SU(3) flavor breaking, the amplitude relations have been obtained. Then using the present data of $\mathcal{B}(D \to P/V/S\ell^+\nu_\ell)$, we have presented a theoretical analysis of the $D \to P/V/S\ell^+\nu_\ell$ decays. Our main results can be summarized as follows.

- $D \to P\ell^+\nu_\ell$ **decays:** Our predictions with the SU(3) flavor symmetry in the C_1 case and the predictions after adding SU(3) flavor breaking contributions in the C_4 case are quite consistent with all present experimental data of $\mathcal{B}(D \to P\ell^+\nu_\ell)$ within 2σ errors. In the C_2 and C_3 cases, our SU(3) flavor symmetry predictions are consistent with all present experimental data except $\mathcal{B}(D^+ \to \pi^0\ell^+\nu_\ell)$ and $\mathcal{B}(D^0 \to \pi^-\ell^+\nu_\ell)$, which are slight larger than their experimental upper limits. The not yet measured $\mathcal{B}(D_s^+ \to \pi^0 e^+\nu_e)$, $\mathcal{B}(D^+ \to \eta'\mu^+\nu_\mu)$, $\mathcal{B}(D_s^+ \to K^0\mu^+\nu_\mu)$, $\mathcal{B}(D_s^+ \to \pi^0\mu^+\nu_\mu)$, $\mathcal{B}(D_s^+ \to \pi^0\tau^+\nu_\tau)$ and the lepton flavor universality parameters have been obtained. Moreover, the forward-backward asymmetries, the lepton-side convexity parameters, the longitudinal (transverse) polarizations of the final charged leptons with two ways of integration for the $D \to P\ell^+\nu_\ell$ decays have been predicted. The q^2 dependence of corresponding differential quantities of the $D \to P\ell^+\nu_\ell$ decays in the C_3 case have been displayed.
- $D \to V\ell^+\nu_\ell$ **decays:** As given in the C_1, C_2 and C_3 cases, our SU(3) flavor symmetry predictions of $\mathcal{B}(D^+ \to \omega e^+\nu_e)$ and $\mathcal{B}(D^0 \to \rho^-\mu^+\nu_\mu)$ are slightly larger than its experimental upper limits, and other SU(3) flavor symmetry predictions are consistent with present data. After considering the SU(3) flavor breaking effects, as given in the C_4 case, all predictions are consistent with present data. The not yet measured or not yet well measured branching ratios of $D^+ \to \phi e^+\nu_e$, $D_s^+ \to \omega e^+\nu_e$, $D^+ \to \phi\mu^+\nu_\mu$, $D_s^+ \to \omega\mu^+\nu_\mu$,

and $D_s^+ \to K^{*0}\mu^+\nu_\mu$ have been predicted. The q^2 dependence of corresponding differential quantities of the $D \to V\ell^+\nu_\ell$ decays in the C_3 case have also been displayed.

- $D \to S\ell^+\nu_\ell$ **decays:** Among 18 $D \to S\ell^+\nu_\ell$ decay modes, only $\mathcal{B}(D_s^+ \to f_0(980)e^+\nu_e)$ has been measured, and this experimental datum has been used to constrain the SU(3) flavor symmetry parameter and then predict other not yet measured branching ratios. Furthermore, the relevant experimental bounds of $\mathcal{B}(D \to S\ell^+\nu_\ell,\ S \to P_1P_2)$ have also been added. The two quark and the four quark scenarios for the light scalar mesons are considered, and the three possible ranges of the mixing angle θ_S in the two quark picture have been analyzed.

The SU(3) flavor symmetry is an approximate approach, and it can still provide very useful information. We have found that the SU(3) flavor symmetry approach works well in the semileptonic $D \to P/V\ell^+\nu_\ell$ decays, and the SU(3) flavor symmetry predictions of the $D \to S\ell^+\nu_\ell$ decays need to be further tested, and our predictions of the $D \to S\ell^+\nu_\ell$ decays are useful for probing the structure of light scalar mesons. According to our predictions, some decay modes could be observed at BESIII, LHCb or BelleII in near future experiments.

CRediT authorship contribution statement

Ru-Min Wang: Investigation, Methodology, Writing – review & editing. **Yue-Xin Liu:** Methodology, Writing – original draft. **Meng-Yuan Wan:** Methodology, Writing – original draft. **Chong Hua:** Investigation, Methodology. **Jin-Huan Sheng:** Formal analysis, Investigation. **Yuan-Guo Xu:** Formal analysis, Writing – review & editing.

Declaration of competing interest

All authors declare that they have no known competing financial interests or personal relationships that could have appeared to influence the work reported in this paper.

Data availability

No data was used for the research described in the article.

Acknowledgements

The work was supported by the National Natural Science Foundation of China, No. 12175088.

References

[1] R.L. Workman, et al., Particle Data Group, Prog. Theor. Exp. Phys. 2022 (2022) 083C01.
[2] D. Melikhov, B. Stech, Phys. Rev. D 62 (2000) 014006, arXiv:hep-ph/0001113 [hep-ph].
[3] H.Y. Cheng, X.W. Kang, Eur. Phys. J. C 77 (2017) 587, erratum: Eur. Phys. J. C 77 (2017) 863, arXiv:1707.02851 [hep-ph].
[4] N.R. Soni, M.A. Ivanov, J.G. Körner, J.N. Pandya, P. Santorelli, C.T. Tran, Phys. Rev. D 98 (2018) 114031, arXiv:1810.11907 [hep-ph].
[5] Q. Chang, X.N. Li, X.Q. Li, F. Su, Y.D. Yang, Phys. Rev. D 98 (2018) 114018, arXiv:1810.00296 [hep-ph].
[6] Q. Chang, X.L. Wang, L.T. Wang, Chin. Phys. C 44 (2020) 083105, arXiv:2003.10833 [hep-ph].
[7] R.N. Faustov, V.O. Galkin, X.W. Kang, Phys. Rev. D 101 (2020) 013004, arXiv:1911.08209 [hep-ph].
[8] P. Ball, Phys. Rev. D 48 (1993) 3190–3203, arXiv:hep-ph/9305267 [hep-ph].
[9] S. Bhattacharyya, M. Haiduc, A. Tania Neagu, E. Firu, Eur. Phys. J. Plus 134 (2019) 37, arXiv:1709.00882 [nucl-ex].

[10] H.B. Fu, L. Zeng, R. Lü, W. Cheng, X.G. Wu, Eur. Phys. J. C 80 (2020) 194, arXiv:1808.06412 [hep-ph].
[11] H.B. Fu, W. Cheng, L. Zeng, D.D. Hu, T. Zhong, Phys. Rev. Res. 2 (2020) 043129, arXiv:2003.07626 [hep-ph].
[12] I.L. Grach, I.M. Narodetsky, S. Simula, Phys. Lett. B 385 (1996) 317–323, arXiv:hep-ph/9605349 [hep-ph].
[13] H.Y. Cheng, C.K. Chua, C.W. Hwang, Phys. Rev. D 69 (2004) 074025, arXiv:hep-ph/0310359 [hep-ph].
[14] Q. Chang, X.N. Li, L.T. Wang, Eur. Phys. J. C 79 (2019) 422, arXiv:1905.05098 [hep-ph].
[15] V. Lubicz, L. Riggio, G. Salerno, S. Simula, C. Tarantino ETM, Phys. Rev. D 98 (2018) 014516, arXiv:1803.04807 [hep-lat].
[16] V. Lubicz, L. Riggio, G. Salerno, S. Simula, C. Tarantino, ETM, erratum: Phys. Rev. D 96 (2017) 054514, Phys. Rev. D 99 (2019) 099902;
erratum: Phys. Rev. D 100 (2019) 079901, arXiv:1706.03017 [hep-lat].
[17] X.G. He, Eur. Phys. J. C 9 (1999) 443, arXiv:hep-ph/9810397.
[18] X.G. He, Y.K. Hsiao, J.Q. Shi, Y.L. Wu, Y.F. Zhou, Phys. Rev. D 64 (2001) 034002, arXiv:hep-ph/0011337.
[19] H.K. Fu, X.G. He, Y.K. Hsiao, Phys. Rev. D 69 (2004) 074002, arXiv:hep-ph/0304242.
[20] Y.K. Hsiao, C.F. Chang, X.G. He, Phys. Rev. D 93 (2016) 114002, arXiv:1512.09223 [hep-ph].
[21] X.G. He, G.N. Li, Phys. Lett. B 750 (2015) 82, arXiv:1501.00646 [hep-ph].
[22] M. Gronau, O.F. Hernandez, D. London, J.L. Rosner, Phys. Rev. D 50 (1994) 4529, arXiv:hep-ph/9404283.
[23] M. Gronau, O.F. Hernandez, D. London, J.L. Rosner, Phys. Rev. D 52 (1995) 6356, arXiv:hep-ph/9504326.
[24] S.H. Zhou, Q.A. Zhang, W.R. Lyu, C.D. Lu, Eur. Phys. J. C 77 (2017) 125, arXiv:1608.02819 [hep-ph].
[25] H.Y. Cheng, C.W. Chiang, A.L. Kuo, Phys. Rev. D 91 (2015) 014011, arXiv:1409.5026 [hep-ph].
[26] M. He, X.G. He, G.N. Li, Phys. Rev. D 92 (2015) 036010, arXiv:1507.07990 [hep-ph].
[27] N.G. Deshpande, X.G. He, Phys. Rev. Lett. 75 (1995) 1703, arXiv:hep-ph/9412393.
[28] S. Shivashankara, W. Wu, A. Datta, Phys. Rev. D 91 (2015) 115003, arXiv:1502.07230 [hep-ph].
[29] R.M. Wang, Y.G. Xu, C. Hua, X.D. Cheng, Phys. Rev. D 103 (2021) 013007, arXiv:2101.02421 [hep-ph].
[30] R.M. Wang, X.D. Cheng, Y.Y. Fan, J.L. Zhang, Y.G. Xu, J. Phys. G 48 (2021) 085001, arXiv:2008.06624 [hep-ph].
[31] Y. Grossman, D.J. Robinson, J. High Energy Phys. 1304 (2013) 067, arXiv:1211.3361 [hep-ph].
[32] Q. Qin, H.n. Li, C.D. Lü, F.S. Yu, Phys. Rev. D 89 (2014) 054006, arXiv:1305.7021 [hep-ph].
[33] H.Y. Jiang, F.S. Yu, Q. Qin, H.n. Li, C.D. Lü, Chin. Phys. C 42 (2018) 063101, arXiv:1705.07335 [hep-ph].
[34] D. Pirtskhalava, P. Uttayarat, Phys. Lett. B 712 (2012) 81, arXiv:1112.5451 [hep-ph].
[35] H.Y. Cheng, C.W. Chiang, Phys. Rev. D 86 (2012) 014014, arXiv:1205.0580 [hep-ph].
[36] M.J. Savage, R.P. Springer, Phys. Rev. D 42 (1990) 1527.
[37] M.J. Savage, Phys. Lett. B 257 (1991) 414.
[38] G. Altarelli, N. Cabibbo, L. Maiani, Phys. Lett. B 57 (1975) 277.
[39] C.D. Lü, W. Wang, F.S. Yu, Phys. Rev. D 93 (2016) 056008, arXiv:1601.04241 [hep-ph].
[40] C.Q. Geng, Y.K. Hsiao, Y.H. Lin, L.L. Liu, Phys. Lett. B 776 (2018) 265, arXiv:1708.02460 [hep-ph].
[41] C.Q. Geng, Y.K. Hsiao, C.W. Liu, T.H. Tsai, Phys. Rev. D 97 (2018) 073006, arXiv:1801.03276 [hep-ph].
[42] C.Q. Geng, Y.K. Hsiao, C.W. Liu, T.H. Tsai, J. High Energy Phys. 1711 (2017) 147, arXiv:1709.00808 [hep-ph].
[43] C.Q. Geng, C.W. Liu, T.H. Tsai, S.W. Yeh, arXiv:1901.05610 [hep-ph].
[44] W. Wang, Z.P. Xing, J. Xu, Eur. Phys. J. C 77 (2017) 800, arXiv:1707.06570 [hep-ph].
[45] D. Wang, arXiv:1901.01776 [hep-ph].
[46] D. Wang, P.F. Guo, W.H. Long, F.S. Yu, J. High Energy Phys. 1803 (2018) 066, arXiv:1709.09873 [hep-ph].
[47] S. Müller, U. Nierste, S. Schacht, Phys. Rev. D 92 (2015) 014004, arXiv:1503.06759 [hep-ph].
[48] L. Zhang, X.W. Kang, X.H. Guo, L.Y. Dai, T. Luo, C. Wang, J. High Energy Phys. 02 (2021) 179, arXiv:2012.04417 [hep-ph].
[49] J. Barranco, D. Delepine, V. Gonzalez Macias, L. Lopez-Lozano, arXiv:1404.0454 [hep-ph].
[50] J. Barranco, D. Delepine, V. Gonzalez Macias, L. Lopez-Lozano, Phys. Lett. B 731 (2014) 36, arXiv:1303.3896 [hep-ph].
[51] A.G. Akeroyd, F. Mahmoudi, J. High Energy Phys. 0904 (2009) 121, arXiv:0902.2393 [hep-ph].
[52] B.A. Dobrescu, A.S. Kronfeld, Phys. Rev. Lett. 100 (2008) 241802, arXiv:0803.0512 [hep-ph].
[53] A.G. Akeroyd, C.H. Chen, Phys. Rev. D 75 (2007) 075004, arXiv:hep-ph/0701078.
[54] S. Fajfer, J.F. Kamenik, Phys. Rev. D 73 (2006) 057503, arXiv:hep-ph/0601028.
[55] S. Fajfer, J.F. Kamenik, Phys. Rev. D 72 (2005) 034029, arXiv:hep-ph/0506051.
[56] S. Fajfer, J.F. Kamenik, Phys. Rev. D 71 (2005) 014020, arXiv:hep-ph/0412140.
[57] A.G. Akeroyd, Prog. Theor. Phys. 111 (2004) 295, arXiv:hep-ph/0308260.
[58] A.G. Akeroyd, S. Recksiegel, Phys. Lett. B 554 (2003) 38, arXiv:hep-ph/0210376.
[59] M.A. Ivanov, J.G. Körner, J.N. Pandya, P. Santorelli, N.R. Soni, C.T. Tran, Front. Phys. 14 (2019) 64401, arXiv:1904.07740 [hep-ph].

[60] X.G. He, Y.J. Shi, W. Wang, Eur. Phys. J. C 80 (2020) 359, arXiv:1811.03480 [hep-ph].
[61] H.Y. Cheng, C.K. Chua, K.C. Yang, Phys. Rev. D 73 (2006) 014017, arXiv:hep-ph/0508104 [hep-ph].
[62] L. Maiani, F. Piccinini, A.D. Polosa, V. Riquer, Phys. Rev. Lett. 93 (2004) 212002, arXiv:hep-ph/0407017 [hep-ph].
[63] L.Y. Dai, X.W. Kang, Ulf-G. Meißner, Phys. Rev. D 98 (2018) 074033, arXiv:1808.05057 [hep-ph].
[64] G. 't Hooft, G. Isidori, L. Maiani, A.D. Polosa, V. Riquer, Phys. Lett. B 662 (2008) 424–430, arXiv:0801.2288 [hep-ph].
[65] J.R. Pelaez, Phys. Rev. Lett. 92 (2004) 102001, arXiv:hep-ph/0309292 [hep-ph].
[66] Y.J. Sun, Z.H. Li, T. Huang, Phys. Rev. D 83 (2011) 025024, arXiv:1011.3901 [hep-ph].
[67] J.A. Oller, E. Oset, Nucl. Phys. A 620 (1997) 438–456, erratum: Nucl. Phys. A 652 (1999) 407–409, arXiv:hep-ph/9702314 [hep-ph].
[68] V. Baru, J. Haidenbauer, C. Hanhart, Y. Kalashnikova, A.E. Kudryavtsev, Phys. Lett. B 586 (2004) 53–61, arXiv:hep-ph/0308129 [hep-ph].
[69] N.N. Achasov, V.V. Gubin, V.I. Shevchenko, Phys. Rev. D 56 (1997) 203–211, arXiv:hep-ph/9605245 [hep-ph].
[70] S. Momeni, M. Saghebfar, Eur. Phys. J. C 82 (2022) 473.
[71] R. Aaij, et al., LHCb, Phys. Rev. D 87 (2013) 052001, arXiv:1301.5347 [hep-ex].
[72] R.L. Jaffe, Phys. Rev. D 15 (1977) 267.
[73] S.S. Gershtein, M.Y. Khlopov, JETP Lett. 23 (338) (1976), IFVE-76-23.
[74] M.Y. Khlopov, Sov. J. Nucl. Phys. 28 (1978) 583.
[75] A. Dery, M. Ghosh, Y. Grossman, S. Schacht, J. High Energy Phys. 03 (2020) 165, arXiv:2001.05397 [hep-ph].
[76] G.S. Yang, H.C. Kim, Phys. Rev. C 92 (2015) 035206, arXiv:1504.04453 [hep-ph].
[77] S. Sasaki, T. Yamazaki, Phys. Rev. D 79 (2009) 074508, arXiv:0811.1406 [hep-ph].
[78] D. Xu, G.N. Li, X.G. He, Int. J. Mod. Phys. A 29 (2014) 1450011, arXiv:1307.7186 [hep-ph].
[79] X.G. He, G.N. Li, D. Xu, Phys. Rev. D 91 (2015) 014029, arXiv:1410.0476 [hep-ph].
[80] M. Tanaka, R. Watanabe, Phys. Rev. D 82 (2010) 034027, arXiv:1005.4306 [hep-ph].
[81] M. Tanaka, Z. Phys. C 67 (1995) 321, arXiv:hep-ph/9411405.
[82] S. Fajfer, J.F. Kamenik, I. Nisandzic, Phys. Rev. D 85 (2012) 094025, arXiv:1203.2654 [hep-ph].
[83] A. Celis, M. Jung, X.Q. Li, A. Pich, J. High Energy Phys. 1301 (2013) 054, arXiv:1210.8443 [hep-ph].
[84] C. Bobeth, G. Hiller, D. van Dyk, J. High Energy Phys. 1007 (2010) 098, arXiv:1006.5013 [hep-ph].
[85] H.B. Li, M.Z. Yang, Phys. Lett. B 811 (2020) 135879, arXiv:2006.15798 [hep-ph].
[86] N.N. Achasov, A.V. Kiselev, Phys. Rev. D 86 (2012) 114010, arXiv:1206.5500 [hep-ph].
[87] N.R. Soni, A.N. Gadaria, J.J. Patel, J.N. Pandya, Phys. Rev. D 102 (2020) 016013, arXiv:2001.10195 [hep-ph].
[88] X. Leng, X.L. Mu, Z.T. Zou, Y. Li, Chin. Phys. C 45 (2021) 063107, arXiv:2011.01061 [hep-ph].
[89] R.M. Wang, Y. Qiao, Y.J. Zhang, X.D. Cheng, Y.G. Xu, arXiv:2301.00090 [hep-ph].
[90] J. Hietala, D. Cronin-Hennessy, T. Pedlar, I. Shipsey, Phys. Rev. D 92 (2015) 012009, arXiv:1505.04205 [hep-ex].
[91] M. Ablikim, et al., BESIII, arXiv:2110.13994 [hep-ex].
[92] M. Ablikim, et al., BESIII, Phys. Rev. Lett. 122 (2019) 062001, arXiv:1809.06496 [hep-ex].
[93] P. Colangelo, F. De Fazio, W. Wang, Phys. Rev. D 81 (2010) 074001, arXiv:1002.2880 [hep-ph].
[94] W. Wang, C.D. Lu, Phys. Rev. D 82 (2010) 034016, arXiv:0910.0613 [hep-ph].
[95] X.D. Cheng, H.B. Li, B. Wei, Y.G. Xu, M.Z. Yang, Phys. Rev. D 96 (2017) 033002, arXiv:1706.01019 [hep-ph].
[96] H.W. Ke, X.Q. Li, Z.T. Wei, Phys. Rev. D 80 (2009) 074030, arXiv:0907.5465 [hep-ph].